PHYSICAL REVIEW D **96,** 094003 (2017)

Transport coefficients of a hot QCD medium and their relative significance in heavy-ion collisions

Sukanya Mitra* and Vinod Chandra†

Indian Institute of Technology Gandhinagar, Palaj, Gandhinagar 382355, Gujarat, India

(Received 16 April 2017; published 9 November 2017)

The main focus of this article is to obtain various transport coefficients for a hot QCD medium that is likely to be produced while colliding two heavy nuclei ultra-relativistically. The technical approach adopted here is the semiclassical transport theory. The away-from-equilibrium linearized transport equation has been set up by employing the Chapman-Enskog technique from the kinetic theory of a many-particle system with a collision term that includes the binary collisions of quarks/antiquarks and gluons. In order to include the effects of a strongly interacting, thermal medium, a quasi-particle description of a realistic hot QCD equation of state has been employed through the equilibrium modeling of the momentum distributions of gluons and quarks with nontrivial dispersion relations while extending the model for finite but small quark chemical potential. The effective coupling for strong interaction has been redefined following the charge renormalization under the scheme of the quasi-particle model. The consolidated effects on transport coefficients are seen to have a significant impact on their temperature dependence. Finally, the relative significances of momentum and heat transfer, as well as the charge diffusion processes in hot QCD, have been investigated by studying the ratios of the respective transport coefficients indicating different physical laws.

DOI: 10.1103/PhysRevD.96.094003

I. INTRODUCTION

The subnucleonic world of partonic substructures (quarks and gluons) has been studied with greater precision in the last few decades by exploring a deconfined state of the nuclear matter at relativistically energetic heavy-ion collider experiments. The experimental facilities at the Relativistic Heavy Ion Collider (RHIC) at Brookhaven National Laboratory and the Large Hadron Collider (LHC) at CERN have provided a fortune of data, which have helped in revealing the thermodynamic and transport properties of the created medium after equilibration. A closer inspection of the experimental observables such as transverse momentum spectra and collective flows of charged hadrons or electromagnetic probes reveals that their quantitative estimates should involve critical dependence upon the transport parameters of the system. This serves as a strong motivation for the quantitative study of the transport coefficients of this exotic medium [quark-gluon plasma (QGP)] that is created while colliding two heavy ions such as Au-Au or Pb-Pb ultra-relativistically, along with a detailed study of their temperature dependences. The transport coefficients under investigation are the shear and bulk viscosities (η and ζ), electrical conductivity (σ_{el}), and thermal conductivity (λ) of the QGP medium at finite but small quark chemical potential, μ_q. Besides providing information about the dissipation and electromagnetic (EM) responses of the medium, these transport parameters give relevant insights about the nature of interaction and nonequilibrium dynamics of the system as well. Earlier predictions of charged hadron elliptic flow from RHIC [1] and their theoretical explanations using dissipative hydrodynamics [2] first provided experimental evidence of the existence of transport processes in the QGP. More recently, a number of ALICE results have reconfirmed the relevance of transport processes [3]. In particular, in the context of the signal properties of charged hadrons and thermally produced particles (photons and dileptons), electromagnetic responses of the QGP medium were also observed to play a vital role, which has been explored in Ref. [4], in the due course of understanding the QGP medium.

To explore the relative importance of these transport parameters and associated physical transport processes, their ratios in the form of known laws (known numbers) in the literature have been investigated. The analysis has been done with semiclassical transport theory, adopting the Chapman-Enskog approach for many-particle systems. The basic approach of determining the transport coefficients in kinetic theory is pursued by comparing the macroscopic and microscopic definitions of thermodynamic flows, as a result of which the particle interactions enter into the expressions of transport coefficients as dynamical inputs. Hence, kinetic theory offers a unique scheme that bridges between the microscopic events of particle interactions and their macroscopic effects (transport phenomena) on the thermodynamic system. The Chapman-Enskog technique has already been employed in

*sukanyam@iitgn.ac.in
†vchandra@iitgn.ac.in

estimating the transport parameters for hadronic systems [5]. In order to initiate the analysis and set up the appropriate transport equation, the very first requirement is the knowledge of local equilibrium momentum distributions of the gluonic and quark degrees of freedom that constitute the QGP. To that end, the modeling of equilibrium momentum distributions of gluons and quarks/antiquarks at vanishing and nonvanishing quark chemical potentials needs to be done in such a way that a realistic equation of state (EOS) for the QGP (such as the lattice QCD EOS) could be mimicked. This has been done by adopting a recently introduced effective quasi-particle model by Chandra and Ravishankar [6,7], where the hot QCD medium effects, present in the equations of state, have been mapped to the equilibrium momentum distributions of quasi-quarks and quasi-gluons containing temperature-dependent quark and gluon effective fugacities. The modified thermodynamic quantities, along with the nontrivial dispersion relation and the effective coupling of the strong interaction within the scope of the quasi-particle model, are observed to influence the temperature dependence of the transport parameters and their ratios significantly. It is to be noted that the validity of quasi-particle descriptions of a hot QCD medium closer to the QCD transition temperature is under question. However, the weak coupling techniques in QCD show nice convergence down to the temperature up to 2 T_c as they agree more or less with lattice QCD predictions on the EOS. In this domain, quasi-particle models could play a prominent role. Keeping this very crucial point in view, such effects models are viable to model the QGP at higher temperatures.

Notably, the velocity gradient between the adjacent fluid layers results in the distortion of momentum distribution within the fluid elements, leading to viscous forces. The viscous coefficients provide a measure of how the microscopic interactions within the system restore the momentum distribution from skewed back to isotropic. The thermal dissipation, occurring due to the temperature gradient over the spatial separations of fluid, is described in terms of thermal conductivity for a system with conserved baryon current density. Besides the dissipative properties, one needs to investigate the electromagnetic (EM) responses in the QGP system, since a considerably strong EM field ($eB \sim m_\pi^2$) is being generated in the early stages of heavy-ion collisions. In order to quantify the impact of the fields on electromagnetically charged QGP, the electrical conductivity plays quite a useful role. It gives a measure of the electric current being induced in the response of the early-stage electric field. In strongly correlated systems like nonrelativistic, ultra-cold atomic Fermi gases or strongly coupled Bose fluids (in particular, liquid helium), and for the QGP medium, the specific shear viscosity (η/s) is observed to have small values, exhibiting near-perfect fluidity of the system [8,9]. The value of the shear viscosity has been constrained by its ratio over the system's entropy density (η/s) by a lower bound of $1/4\pi$, following the uncertainty principle and substantiated using anti–de Sitter space/conformal field theory (AdS/CFT) correspondence [10]. The agreement of the hydrodynamic description with the experimental data in Ref. [2] also confirms this small value ($\eta/s = 2/4\pi$) of shear viscous coefficient, which appears to be consistent with the values extracted directly from experiments [11] and lattice simulations [12] as well. The magnitude of bulk viscosity ζ is found to be quite small as compared to the shear viscosity η, due to which early viscous hydrodynamic simulations ignored bulk viscosity for simplicity [13]. Although it vanishes for a conformal fluid or massless QGP on the classical level, quantum effects break the conformal symmetry of QCD and generate a nonzero bulk viscosity even in the massless QGP phase, as recently shown by the lattice results [14] in the $SU(3)$ pure gauge theory.

Following the general argument that the QCD to hadron gas transition is a crossover, η/s shows a minimum near T_c, the critical temperature, close to the lower bound [15,16], whereas the bulk viscosity to entropy density ratio ζ/s shows large values around T_c [17,18]. Finally, at FAIR energies and in the low-energy runs at RHIC, where the baryon chemical potential will be significant, thermal conductivity (λ) is expected to play important roles in the hydrodynamic evolution of the system. In Ref. [19], the thermal conductivity is shown to diverge at the critical point and used to study the impact of hydrodynamic fluctuations on experimental observables. As a consequence of the strong electromagnetic field generated in the early stages of heavy-ion collisions, the produced matter, after thermalization, involves a non-negligible electrical conductivity σ_{el}. In Ref. [20], nontrivial time dependence of the electromagnetic fields is observed to be sensitive to this finite electrical conductivity. In Ref. [21], the electromagnetic responses in the plasma fireball are demonstrated in the presence of a realistic σ_{el}, demanding a finite value of electrical conductivity in the QGP system.

The relative behavior of these transport parameters leads to a comparative measure between different thermodynamic dissipations and electromagnetic responses. The mutual ratios between η, λ, and σ_{el} can reflect the competition between momentum transport, heat transport, and charge transport in the medium, respectively. We start with the Wiedemann-Franz law, which states that the thermal conductivity of a system is proportional to its electrical conductivity times the bulk temperature (T) of the system, such that $\lambda/(\sigma_{el}T)$ is a constant of temperature. The ratio is known as the Lorenz number, which for most of the system including metals is independent of temperature, depending only on the fundamental constants. In Ref. [22], a breakdown of the Wiedemann-Franz law has been reported for electron-hole plasma in graphene, indicating the signature of a strongly coupled Dirac fluid. Recently in Ref. [23], a violation of the Wiedemann-Franz law has also been reported for the two-flavor quark matter described by the

Nambu–Jona-Lasinio (NJL) model. In the same context, it is interesting to look into the behavior of this law in the strongly interacting QGP medium as well. Next, we focus on the relative behaviors of viscous and thermal dissipation. From AdS/CFT studies of strongly coupled thermal gauge theories in the framework of the gauge-gravity duality, a value of the ratio between shear viscosity and thermal conductivity has been reported [24], providing an analogue of the Wiedemann-Franz law between momentum transport and heat transport. For a system with finite chemical potential μ, the ratio states $\frac{\lambda\mu^2}{\eta T_H} = 8\pi^2$, where T_H is the Hawking temperature. It is more customary to express the relative importance of kinematic viscosity or shear viscosity and thermal conductivity in a dimensionless ratio called the Prandtl number (Pr), given by $\mathrm{Pr} = \eta c_p/\rho\lambda$, where c_p is the specific heat at constant pressure of the system and ρ is the mass density of the system. In a nonrelativistic conformal holographic fluid, this number is estimated to be $\mathrm{Pr} = 1$, from AdS/CFT computations [25]. In Ref. [26], the Prandtl number is estimated to be $\mathrm{Pr} = 2/3$ for a dilute atomic Fermi gas, which agrees with the classical gas result. Finally, we mention the relative behavior between shear viscosity and electrical conductivity, which characterizes the relative importance of momentum diffusion and charge diffusion in an electromagnetically charged system that undergoes dissipation. We can specify this comparison by observing the ratio of two dimensionless quantities, $(\eta/s)/(\sigma_{el}/T)$. Since the electromagnetic responses are mostly carried by the charged components of the system—i.e., by the quarks in a strongly interacting QGP (although the diffusion flows of quarks and gluons are constrained to be coupled with each other, so that the gluon interaction rate in effect enters into the expression of electrical conductivity), whereas both quarks and gluons participate in momentum transport—the shear viscosity should dominate over the electrical conductivity as predicted by Ref. [27] for a strongly interacting QGP system. These physical laws and the associated ratios of transport parameters, by providing useful information about the dynamics and relative responses about the system, are instructive in looking again for the QGP system, which is one of the major motivations of this work.

In order to provide the spectrum of the theoretical estimations of these transport quantities, we need to review the state-of-the-art developments in recent literature. There are a number of estimations of the viscosities employing the transport theory approach, utilizing the kinetic theory of a many-particle system [28–38]. Under the application of Kubo formalism, the QGP viscosities have also been obtained by evaluating the correlation functions using linear response theory in Ref. [39]. Describing the in-medium constituent quark interactions under the scheme of the NJL model, both the shear and bulk viscous coefficients have been estimated in Ref. [40]. The quasi-particle approach, introduced in order to describe the hot QCD medium, has been employed to estimate the viscosities as well [41,42]. The temperature dependences of η and ζ have been constrained from hydrodynamic simulations and by comparison with the experimental data in Refs. [43–45]. Molecular dynamics simulations have been employed in Ref. [46] to extract the shear viscosity to entropy density ratio for a strongly coupled QGP. Quite a few times, the viscous coefficients are being analyzed from holographic predictions as well. These viscous parameters are studied in great detail in recent AdS/CFT-based literature employing holographic QCD models [47]. In comparison to the estimations of viscosities, the study of thermal conductivity has received much less attention in the current scenario. However, a few estimated values of λ are available in works like Refs. [48–50]. Electrical conductivity, which is turning out to be an effective signature of electromagnetic responses in strongly interacting systems, has attained a lot of interest recently. In the strongly coupled QGP, the relativistic transport theory, the dynamical quasi-particle model (DQPM), and the maximum entropy method (MEM) have found a number of applications to estimate the value and temperature dependence of σ_{el} [27,51–57]. From the soft photon spectrum in heavy-ion collisions, σ_{el} has been extracted in Ref. [58]. Quite a considerable number of estimations of σ_{el} are available from lattice QCD computations as well [59–65]. Finally, a number of holographic estimations have been proposed for both thermal and electrical conductivities in Ref. [66].

The manuscript is organized as follows: Section II includes the formal developments of the transport theory, containing the quasi-particle description of a hot QCD medium, the evaluation and temperature behavior of thermal relaxation times of quarks and gluons within the medium, and the details on the estimations of the transport coefficients. The results regarding the transport coefficients and the physical laws concerning their ratios have been provided in Sec. III. The obtained results are discussed in Sec. IV. Finally, in Sec. V, the article has been summarized while providing possible outlooks of the work.

II. FORMALISM: TRANSPORT THEORY

The determination of transport coefficients for a hot QCD system requires modeling of the system away from equilibrium. Their determination can be done within two equivalent approaches: viz., the correlator technique in QCD using the Green-Kubo formula, and the semiclassical transport theory (Chapman-Enskog or Grad's 14 method). The present analysis is done following the latter approach. To initiate the formalism, an appropriate modeling of the equilibrium, isotropic momentum distributions of gluons and quark-antiquarks in the hot QCD medium at vanishing or nonvanishing baryon density (whatever be the case), must be provided. This could be systematically done by adopting an effective modeling of the hot QCD medium effects, encoded in the interacting QCD/QGP equations of

state. To that end, the well-accepted effective fugacity quasi-particle (EQPM) proposed by Chandra and Ravishankar [6,7,67] serves the current purpose which has been discussed below. The quasi-particle modeling of the system properties is followed by the estimations of the essential ingredients, such as the thermal relaxation times of interacting partons and other related quantities that are necessary while determining various transport coefficients under consideration here. Finally, the complete formalism for extracting the transport coefficients is presented with all the required mathematical details below.

A. Effective modeling of momentum distributions of gluons and matter sector

The QCD medium at high temperature can conveniently be realized in terms of its effective quasi-particle degrees of freedom—viz., the quasi-gluons and quasi–quarks/antiquarks with nontrivial dispersion relations. There have been several quasi-particle models proposed over the last few decades to describe the hot QCD equations of state in terms of noninteracting or weakly interacting effective gluons and effective quarks and antiquarks. The effective mass models [68] and the effective mass models with Polyakov loops [69] describe the medium effects in terms of effective thermal mass or effective coupling in the medium. In these models, the thermodynamic consistency condition needs to be handled carefully, sometimes by introducing a few additional temperature-dependent parameters. Another set of these models includes the NJL (Nambu–Jona-Lasinio) and the PNJL (Polyakov loop extended Nambu–Jona-Lasinio)-based effective models [70]. The EQPM, which has been employed here, is described below in detail.

1. The EQPM and its extension to finite quark chemical potential

The EQPM models the hot QCD medium effects in terms of effective quasi-partons (quasi-gluons, quasi–quarks/antiquarks). The main idea is to map the hot QCD medium effects present in the hot QCD EOSs, computed within either improved perturbative QCD (pQCD) or lattice QCD simulations, onto the effective equilibrium distribution functions for the quasi-partons. The EQPM for the QCD EOS at $O(g^5)$ (EOS1) and $O(g^6\ln(1/g)+\delta)$ (EOS2), along with a recent $(2+1)$-flavor lattice QCD EOS (LEOS) [71] at physical quark masses, has been exploited in the present manuscript. Note that there are more recent lattice results with the improved hot QCD actions and refined lattices [72], for which we need to look at the model again with a specific set of lattice data (specifically to define the effective gluonic degrees of freedom). Therefore, we will stick to the set of lattice data utilized in the model described in Ref. [7] and leave the issue for further investigations in the near future.

In either of these EOSs, the form of the quasi-parton equilibrium distribution functions, $f_{eq}\equiv\{f_g, f_{q,\bar{q}}\}$ (describing the strong-interaction effects in terms of effective fugacities $z_{g,q}$), can be written as

$$f_{g/q}=\frac{z_{g/q}\exp[-\beta E_p]}{(1\mp z_{g/q}\exp[-\beta E_p])}, \tag{1}$$

where $E_p=|\vec{p}|$ for the gluons and $\sqrt{|\vec{p}|^2+m_q^2}$ for the quarks/antiquarks (m_q denotes the mass of the quarks). The parameter $\beta=T^{-1}$ denotes the inverse of the temperature, $\nu_g=2(N_c^2-1)$ denotes the gluonic degrees of freedom, and $\nu_q=\nu_{\bar{q}}=2N_cN_f$ are the quark-antiquark degrees of freedom for $SU(N_c)$ with N_f the number of flavors. Since the model is valid in the deconfined phase of QCD (beyond T_c), the mass of the light quarks can be neglected while comparing it with the temperature. Noteworthily, EOS1, which is fully perturbative, is proposed by Arnold and Zhai [73,74] and by Zhai and Kastening [75]; EOS2, which is at $O(g^6\ln(1/g)+\delta)$, is determined by Kajantie *et al.* [76] while incorporating contributions from nonperturbative scales such as gT and g^2T. In the case of vanishing baryon density, $f_q\equiv f_{\bar{q}}$.

It is important to note that these effective fugacities $z_{g/q}$ are not merely temperature-dependent parameters that encode the hot QCD medium effects; they lead to a nontrivial dispersion relation in both the gluonic and quark sectors as

$$\omega_{g/q}=E_p+T^2\partial_T ln(z_{g/q}), \tag{2}$$

where $\omega_{g,q}$ denote the quasi-gluon and quasi-quark dispersions (single-particle energy), respectively. The second term on the right-hand side of Eq. (2) encodes the effects from collective excitations of the quasi-partons.

The extension of the model to finite baryon/quark chemical potential is quite straightforward. This could be done by introducing the quark-chemical potentials (μ_q) in the momentum distributions in the matter sector as

$$f_{q/\bar{q}}=\frac{z_q\exp[-\beta(E_p\mp\mu_q)]}{(1+z_q\exp[-\beta(E_p\mp\mu_q)])}. \tag{3}$$

It is important to note that the temperature dependences of the effective fugacities, z_g, z_q, are set while implementing the EOS1, EOS2, and LEOS in terms of EQPM. In other words, while extending the EQPM for finite but small ($\mu_q/T\ll 1$) baryon densities, the same expressions for z_g and z_q have been employed so that one can get the correct limit in the case where $\mu_q=0$. The effective fugacities z_g, z_q are not related with any conserved number current in the hot QCD medium. They have merely been introduced to encode the hot QCD medium effects in the EQPM. The physical interpretation of z_g and z_q emerges from the above mentioned nontrivial dispersion relations. The modified part of the energy dispersions in Eq. (2) leads to the trace anomaly (interaction measure) in hot QCD and takes care

of the thermodynamic consistency condition. It is straightforward to compute gluon and quark number densities and all the thermodynamic quantities such as energy density, entropy, enthalpy, etc., by realizing the hot QCD medium in terms of an effective grand canonical system [6,7]. Furthermore, these effective fugacities lead to a very simple interpretation of hot QCD medium effects in terms of an effective virial expansion. Note that $z_{g,q}$ scales with T/T_c, where T_c is the QCD transition temperature. For the current analysis, T_c has been taken to be 170 MeV. All the relevant thermodynamic quantities such as energy density, number density, pressure, entropy density, speed of sound, heat capacity, etc., could be straightforwardly obtained in terms of f_g, $f_{q,\bar{q}}$ following their basic definitions.

2. Charge renormalization and effective coupling at finite T and μ_q

In contrast to the effective mass models where the effective mass is motivated from the mass renormalization in the hot QCD medium, the EQPM is based on the charge renormalization in high-temperature QCD. This could be realized by computing the expression for the Debye mass in the medium following its definition that is derived in semiclassical transport theory [77] as

$$m_D^2 = 4\pi\alpha_s(T,\mu_q)\left(-2N_c\int\frac{d^3p}{(2\pi)^3}\partial_p f_g(\vec{p}) - N_f\int\frac{d^3p}{(2\pi)^3}\partial_p(f_q(\vec{p})+f_{\bar{q}}(\vec{p}))\right), \tag{4}$$

where $\alpha_s(T)$ is the QCD running coupling constant at finite temperature and chemical potential.

After performing the momentum integral and substituting the quasi-parton distribution function from Eq. (1) to Eq. (4), we are left with the expression of Debye mass within the scheme of the EQPM model with finite quark chemical potential, up to the order $O(\tilde{\mu_q}^2)$ (since $\tilde{\mu_q}^2 \ll 1$):

$$m_D^2 = 4\pi\alpha_s(T,\mu_q)T^2\left\{\left(\frac{2N_c}{\pi^2}\text{PolyLog}[2,z_g] - \frac{2N_f}{\pi^2}\text{PolyLog}[2,-z_q]\right) + \tilde{\mu_q}^2\frac{N_f}{\pi^2}\frac{z_q}{1+z_q}\right\}. \tag{5}$$

The Debye mass here reduces to the leading-order HTL expression in the limit $z_{g,q}\to 1$ (ideal EoS: noninteracting ultra-relativistic quarks and gluons)

$$m_D^2(\text{HTL}) = 4\pi\alpha_s(T,\mu_q)T^2\left\{\left(\frac{N_c}{3}+\frac{N_f}{6}\right)+\tilde{\mu_q}^2\frac{N_f}{2\pi^2}\right\}. \tag{6}$$

From Eqs. (5) and (6), the effective coupling can be defined as

$$\alpha_{\text{eff}}(T,\mu_q) = \alpha_s(T,\mu_q) \times\left[\frac{\left\{\frac{2N_c}{\pi^2}\text{PolyLog}\left[2,z_g\right]-\frac{2N_f}{\pi^2}\text{PolyLog}[2,-z_q]\right\}}{\left\{\frac{N_c}{3}+\frac{N_f}{6}\right\}+\tilde{\mu_q}^2\left\{\frac{N_f}{2\pi^2}\right\}} + \tilde{\mu_q}^2\frac{\left\{\frac{N_f}{\pi^2}\frac{z_q}{1+z_q}\right\}}{\left\{\frac{N_c}{3}+\frac{N_f}{6}\right\}+\tilde{\mu_q}^2\left\{\frac{N_f}{2\pi^2}\right\}}\right]. \tag{7}$$

The behavior of the ratio m_D^2/T^2 as a function of temperature (T/T_c) for various EOSs and finite μ_q is depicted in Fig. 1. As expected, the finite but small μ_q effects are quite visible at lower temperatures, which are merging with the zero quark chemical potential cases at higher temperatures. This is seen to be valid for all of the three EOSs considered here. The medium effects (thermal) manifested through the temperature-dependent $z_{g,q}$ play the crucial role in modulating the quantity m_D^2/T^2 as a function of temperature.

There are only three free functions (z_g, z_q, and $\tilde{\mu}_q$) in the EQPM employed here. The first two depend on the chosen EOS. For EOS1 and EOS2 employed in the present case, these functions are obtained in Ref. [6] and are continuous functions of T/T_c. On the other hand, for LEOS, they are defined in terms of eight parameters obtained in Ref. [7] (See Table I of Ref. [7]). The quantity $\tilde{\mu_q}$ is chosen to be 0.0 and 0.1 GeV throughout our analysis. In addition, the effective coupling mentioned above depends on the QCD running coupling constant $g(T,\mu_q)=\sqrt{4\pi\alpha_s}$, that explicitly depends upon how we fix the QCD renormalization scale at finite temperature and μ_q, and up to what order we define $g(T,\mu_q)$. Henceforth, these are the only quantities that need to be supplied throughout the analysis here.

Notably, the EQPM employed here has been remarkably useful in understanding the bulk and the transport properties of the QGP in heavy-ion collisions [78]. Before

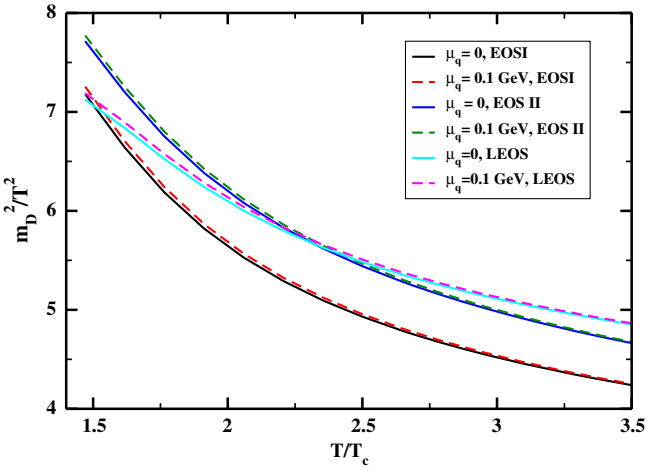

FIG. 1. Effective coupling constant using various EOSs as a function of T/T_c.

discussing the formalism for estimations of thermal relaxation times of the constituent gluons and quarks, it is important to highlight the utility of quasi-particle models in the context of understanding the bulk and transport properties of the hot QCD/QGP medium created out of the heavy-ion collisions. As already mentioned, transport parameters of the QGP have been estimated, employing various quasi-particle models in Refs. [41,42,78–80]. Note that Ref. [80] offers the estimation of η and ζ for pure gluon plasma employing the effective mass quasi-particle model. On the other hand, Ref. [42] reports estimations for both the gluonic as well as the matter sector. References [79,81] present the quasi-particle estimations of η and ζ in the hadronic sector. The thermal conductivity has also been studied, in addition to the viscosity parameters [79], within the effective mass model at finite baryon density.

If EQPM is analyzed in contrast to the effective mass models (with lattice QCD data for the EOS interpreted in terms of the effective thermal gluon mass and the effective thermal quark mass), the effective fugacity or the modified dispersions for the quasi-gluons and quarks/antiquarks cannot simply be related to the effective mass. This is because at the level of dispersions, it leads to a momentum-dependent masslike parameter which is not the same as the effective mass. This makes it completely distinct from effective-mass-based models. However, the effective fugacities are not the effective masses, and they can only be interpreted as effective mass in some limiting case $[p \ll T^2\partial_T \ln(z_{g,q})]$ (as we shall see later, this cannot be achieved in the present case). The effective fugacities have an explanation in terms of a virial expansion [6]. Another fundamental difference is in terms of realizing the thermodynamic consistency condition in a hot QCD medium. Unlike effective mass models, in which one needs to add terms concerning the mean field contribution to the kinetic theory definition of the energy-momentum tensor, $T^{\mu\nu}$ (which modifies the expressions for the energy density and pressure, etc.) [82–84]; in the case of EQPM, the modified dispersions take care of the thermodynamic consistency. Therefore, the modified $T^{\mu\nu}$ could be obtained by simply generalizing its basic kinetic theory definition as discussed below.

The first step towards setting up an effective kinetic theory with EQPM is the microscopic (kinetic theory) definition of the energy-momentum tensor, $T^{\mu\nu}$, which leads to correct expressions for the thermodynamic quantities such as energy density, through $u_\mu T^{\mu\nu} u_\nu = \epsilon_Q$ in the local rest frame. Here, ϵ_Q is the energy density obtained from EQPM in terms of the dispersion relation ω as

$$\epsilon_Q = \sum_{k=g,q,\bar{q}} \int \frac{d^3\vec{p}}{(2\pi)^3} \omega_k f_k, \tag{8}$$

where f_g, $\omega_{g,q}$, $f_{q,\bar{q}}$ are given in Eqs. (1)–(3), respectively. This expression yields the trace anomaly in hot QCD.

This could be achieved by generalizing the definition of $T^{\mu\nu}$ in any arbitrary frame, as

$$T^{\mu\nu} = \sum_{k=g,q,\bar{q}} \int \frac{d^3\vec{p}}{(2\pi)^3 \omega_k} p_k^\mu p_k^\nu f_k(\vec{p},\vec{r}), \tag{9}$$

where $p_k^\mu \equiv (\omega_k, \vec{p})$ is the four-momentum of the effective gluons and the effective quark-antiquarks, and $f_k(\vec{p},\vec{r})$ in general contains nonequilibrium terms. The expression for $T^{\mu\nu}$ for the EQPM has been discussed earlier in Ref. [42], in terms of $T^{\mu\nu}$ of the undressed (bare) degrees of freedom of the hot QCD and terms containing the quasi-particle dispersions. This suggests either that no additional mean-field term is required, as the modified dispersions of the quasi-particles in our case take care of the thermodynamic consistency condition—or, that if it is at all required at the level of developing second-order dissipative hydrodynamics from the effective kinetic theory with EQPM (as discussed in the Appendix), it must not modify the definitions of thermodynamic quantities.

Setting up transport theory (for the first-order transport coefficients) within the EQPM is quite simple, as the bare four-momenta need to be changed by the quasi-particles mentioned earlier. Notably, the presence of modified dispersion relations appearing in the transport equation is obtained by the action of the drift operator on f_{eq} through the temperature derivative [85]. The effective transport equation is discussed in the following subsections.

B. Thermal relaxation times

As mentioned earlier, the microscopic interactions between the constituents of the system provide the dynamical inputs for different transport coefficients. Here, it is done by introducing the thermal relaxation times of the partons, which in turn introduce the transport cross sections to the expressions of the transport coefficients.

In order to define the thermal relaxation times for quasi–quarks/antiquarks and gluons, we start with the relativistic transport equation of the momentum distribution functions of the constituent partons in an out-of-equilibrium, multicomponent system that describes the binary elastic process $p_k + p_l \to p_k' + p_l'$:

$$p_k^\mu \partial_\mu f_k = \sum_{l=1}^{N} C_{kl}[f_k, f_l], \qquad [k = 1, 2, \ldots N]. \tag{10}$$

Here f_k is the single-particle distribution function for the kth species, which depends upon the particle four-momentum p_k and the four-spacetime coordinates x. Here, the right-hand side of Eq. (10) denotes the collision term that quantifies the rate of change of f_k. For each l, $C_{kl}[f_k, f_l]$ defines the collision contribution due to the scattering of the kth particle, with the lth one given in the following manner [33]:

$$C_{kl}[f_k,f_l]=\frac{1}{2}\frac{\nu_l}{2}\int d\Gamma_{p_l}d\Gamma_{p'_k}d\Gamma_{p'_l}\delta^4(p_k+p_l-p'_k-p'_l)\times(2\pi)^4[f_k(p'_k)f_l(p'_l)\{1\pm f_k(p_k)\}\{1\pm f_l(p_l)\}-f_k(p_k)f_l(p_l)\{1\pm f_k(p'_k)\}\{1\pm f_l(p'_l)\}]\times\langle|M_{k+l\to k+l}|^2\rangle. \quad (11)$$

The phase-space factor is given by the notation $d\Gamma_{p_i}=\frac{d^3\vec{p}_i}{(2\pi)^3 2\omega_i}$, as ω_k is the energy of the scattered particle (of the kth species). The overall $\frac{1}{2}$ factor appears due to the symmetry in order to compensate for the double-counting of final states that occurs by interchanging p'_k and p'_l. ν_l is the degeneracy of the second particle that belongs to the lth species. Equations (10) and (11), with f_k identified with quasi-particle momentum distribution functions given in Eq. (1), lead to conservations of the number current and energy momentum tensor (with the zeroth and first moments of the transport equation, respectively). This is due to the fact that the summation invariant that is followed by particle-number and four-momentum conservation in the case of binary elastic collisions remains intact while employing the EQPM, since the effective fugacities are free from momentum dependence.

In the present case up to next-to-leading order, the out-of-equilibrium distribution function is constructed as follows:

$$f_k=f_k^0+\delta f_k=f_k^0+f_k^0(1\pm f_k^0)\phi_k, \quad (12)$$

where the nonequilibrium part δf_k of the distribution function is quantified by the deviation function ϕ_k. The distribution functions of the quasi-partons at local thermal equilibrium are given by Eq. (1).

The simplest method of linearizing the transport equation (10) is to replace the collision term with the rate of change of the distribution function over the thermal relaxation time τ_k which is needed by the out-of-equilibrium distribution function to restore its equilibrium value, such that the transport equation becomes

$$\frac{df_k}{dt}=-\frac{\delta f_k}{\tau_k}=-\frac{(f_k-f_k^0)}{\tau_k}. \quad (13)$$

Consequently, the collision term becomes

$$\sum_{l=1}^{N}C_{kl}[f_k,f_l]=-\omega_k\frac{\delta f_k}{\tau_k}=-\omega_k\frac{f_k^0(1\pm f_k^0)\phi_k}{\tau_k}. \quad (14)$$

Putting (12) into the right-hand side of (11) by assuming that the distribution functions of the particles other than the scattered one are very close to equilibrium and comparing with Eq. (14), the relaxation time finally becomes as the inverse of the reaction rate Γ_k of the respective processes [86]:

$$\tau_k^{-1}\equiv\Gamma_k=\sum_{l=1}^{N}\frac{\nu_l}{2}\frac{1}{2\omega_k}\int d\Gamma_{p_l}d\Gamma_{p'_k}d\Gamma_{p'_l}\delta^4(p_k+p_l-p'_k-p'_l)\times(2\pi)^4\langle|M_{k+l\to k+l}|^2\rangle\frac{f_l^0(1\pm f_k'^0)(1\pm f_l'^0)}{(1\pm f_k^0)}. \quad (15)$$

Clearly, the distribution function of final-state particles is given by primed notation.

Simplifying τ_k utilizing the δ function, we finally obtain its expression in the center-of-momentum frame of particle interaction as

$$\tau_k^{-1}=\Gamma_k=\sum_{l=1}^{N}\nu_l\int\frac{d^3\vec{p}_l}{(2\pi)^3}d(\cos\theta)\frac{d\sigma}{d(\cos\theta)}\frac{f_l^0(1\pm f_k'^0)(1\pm f_l'^0)}{(1\pm f_k^0)}, \quad (16)$$

where θ is the scattering angle in the center-of-momentum frame and σ is the interaction cross section for the respective scattering processes. Now, in terms of the Mandelstam variables s, t, and u, the expression for τ_k can be reduced simply to

$$\tau_k^{-1}=\Gamma_k=\sum_{l=1}^{N}\nu_l\int\frac{d^3\vec{p}_l}{(2\pi)^3}dt\frac{d\sigma}{dt}\frac{f_l^0(1\pm f_k'^0)(1\pm f_l'^0)}{(1\pm f_k^0)}. \quad (17)$$

The differential cross section relates the scattering amplitudes as $\frac{d\sigma}{dt}=\frac{\langle|M|^2\rangle}{16\pi s^2}$. The QCD scattering amplitudes for $2\to2$ binary, elastic processes are taken from Ref. [87], that are averaged over the spin and color degrees of freedom of the initial states and summed over the final states. The inelastic processes like $q\bar{q}\to gg$ have been ignored in the present case, because they do not have a forward peak in the differential cross section, and thus their contributions will presumably be small compared to the elastic ones.

Now, in order to take into account the small-angle scattering scenario that results in divergent contributions from t-channel diagrams of QCD interactions, a transport weight factor $(1-\cos\theta)=\frac{2tu}{s^2}$ has been introduced in the interaction rate [32]. Furthermore, considering the momentum transfer $q=|\vec{p}_k-\vec{p}'_k|=|\vec{p}_l-\vec{p}'_l|$ is not too large, we can make the assumptions $f_k^0\cong f_k'^0$ and $f_l^0\cong f_l'^0$ [88] to finally obtain

$$\tau_k^{-1}=\Gamma_k=\sum_{l=1}^{N}\nu_l\int\frac{d^3\vec{p}_l}{(2\pi)^3}f_l^0(1\pm f_l^0)\int dt\frac{d\sigma}{dt}\frac{2tu}{s^2}. \quad (18)$$

This additional transport factor changes the infrared and ultraviolet behavior of the interaction rate quite

significantly. Due to the inclusion of this term, all the higher-order divergences reduce to simple logarithmic singularities which can be simply handled by putting a small-angle cutoff in the integration limit. In the integration involving t-channel diagrams from where the infrared logarithmic singularity appears, the limit of integration is restricted from $-s$ to $-k^2$ in order to avoid those divergent results using the cutoff $k^2 = g^2T^2$ as an infrared regulator. Here $g^2 = 4\pi\alpha_s$, with α_s being the coupling constant of strong interaction, as already mentioned in Sec. I.

Finally, after pursuing the angular integration in (18), we are left with the thermal relaxation times of the quark, antiquark, and gluon components in a QGP system in the following way:

$$\tau_g^{-1} = \left\{\nu_g \int \frac{d^3\vec{p_g}}{(2\pi)^3} f_g^0(1+f_g^0)\right\}\left[\frac{9g^4}{16\pi\langle s\rangle_{gg}}\left\{ln\frac{\langle s\rangle_{gg}}{k^2} - 1.267\right\}\right] + \left\{\nu_q \int \frac{d^3\vec{p_q}}{(2\pi)^3} f_q^0(1-f_q^0)\right\}\left[\frac{g^4}{4\pi\langle s\rangle_{gq}} \times \left\{ln\frac{\langle s\rangle_{gq}}{k^2} - 1.287\right\}\right] + \left\{\nu_{\bar{q}} \int \frac{d^3\vec{p_{\bar{q}}}}{(2\pi)^3} f_{\bar{q}}^0(1-f_{\bar{q}}^0)\right\} \times \left[\frac{g^4}{4\pi\langle s\rangle_{g\bar{q}}}\left\{ln\frac{\langle s\rangle_{g\bar{q}}}{k^2} - 1.287\right\}\right], \tag{19}$$

$$\tau_{q,(\bar{q})}^{-1} = \left\{\nu_g \int \frac{d^3\vec{p_g}}{(2\pi)^3} f_g^0(1+f_g^0)\right\}\left[\frac{g^4}{4\pi\langle s\rangle_{q(\bar{q})g}}\left\{ln\frac{\langle s\rangle_{q(\bar{q})g}}{k^2} - 1.287\right\}\right] + \left\{\nu_q \int \frac{d^3\vec{p_q}}{(2\pi)^3} f_q^0(1-f_q^0)\right\}\left[\frac{g^4}{9\pi\langle s\rangle_{q(\bar{q})q}} \times \left\{ln\frac{\langle s\rangle_{q(\bar{q})q}}{k^2} - 1.417\right\}\right] + \left\{\nu_{\bar{q}} \int \frac{d^3\vec{p_{\bar{q}}}}{(2\pi)^3} f_{\bar{q}}^0(1-f_{\bar{q}}^0)\right\} \times \left[\frac{g^4}{9\pi\langle s\rangle_{q(\bar{q})\bar{q}}}\left\{ln\frac{\langle s\rangle_{q(\bar{q})\bar{q}}}{k^2} - 1.417\right\}\right], \tag{20}$$

where $\langle s\rangle_{kl} = 2\langle p_k\rangle\langle p_l\rangle$ is the thermal average value of s, with $\langle p_k\rangle = \frac{\int \frac{d^3\vec{p_k}}{(2\pi)^3}|\vec{p_k}|f_k^0}{\int \frac{d^3\vec{p_k}}{(2\pi)^3} f_k^0}$. Clearly, in order to account for a hot QCD medium, the quasi-particle effects must be invoked in the expressions of these thermal relaxation times obtained so far. As discussed in Sec. II A, the distribution functions of quarks and gluons and the coupling g will carry the quasi-particle descriptions accordingly. Since the cutoff parameter k also depends upon g, and the thermal average of s includes $f_{g,q,\bar{q}}^0$, they will reflect the hot QCD equation-of-state effect as well. Following the definition of the equilibrium distribution function of quarks and gluons from Eq. (1), within the quasi-particle framework, the thermal averages of gluon and quark momenta are obtained as

$$\langle p_g\rangle = 3T\frac{\text{PolyLog}[4, z_g]}{\text{PolyLog}[3, z_g]}, \tag{21}$$

$$\langle p_{q/\bar{q}}\rangle = 3T\Big\{\text{PolyLog}[4,-z_q] \pm \tilde{\mu_q}\text{PolyLog}[3,-z_q] + \frac{(\tilde{\mu_q})^2}{2}\text{PolyLog}[2,-z_q]\Big\}\Big/\Big\{\text{PolyLog}[3,-z_q] \pm \tilde{\mu_q}\text{PolyLog}[3,-z_q] - \frac{(\tilde{\mu_q})^2}{2}ln(1+z_q)\Big\}, \tag{22}$$

respectively. The degeneracy factors used are $\nu_g = 2\times 8 = 16$ and $\nu_q = \nu_{\bar{q}} = 2\times N_c \times N_f$, where N_f and N_c are the quark numbers of flavors and colors, respectively. From the above analysis, it turns out that the thermal relaxation times at a particular μ_q follow the form

$$\tau_{q/\bar{q},g}^{-1} \sim T\alpha_s^2 ln\left\{\frac{1}{\alpha_s}\right\}. \tag{23}$$

In Figs. 2 and 3, the temperature dependences of the thermal relaxation times of quasi-gluons and quarks, obtained from Eqs. (19) and (20), respectively, have been plotted as a function of T/T_c. The temperature dependence of τ for both the gluonic and quark components is observed to exhibit an obvious decreasing trend with increasing temperature, revealing that the enhanced interaction rates at higher temperatures make the thermal quarks and gluons restore down their equilibrium faster. We observe that at a particular temperature, τ_q is quantitatively little greater than τ_g, indicating stronger interaction rates of the gluonic part. The order of magnitude of the relaxation times and the fact that τ_q is larger than τ_g agree with the work given in Ref. [29].

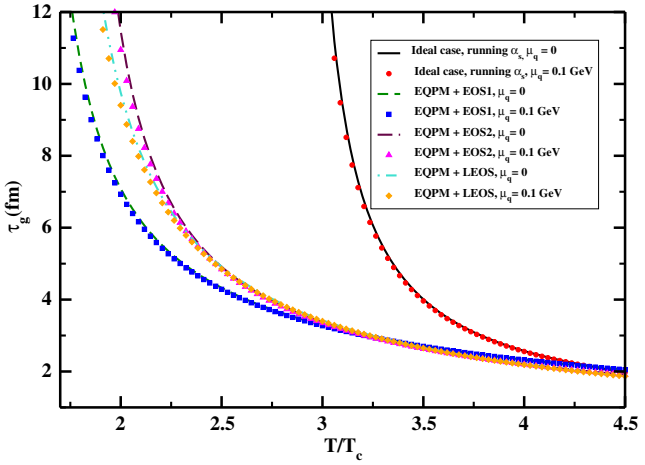

FIG. 2. Thermal relaxation times for gluons using various EOSs as a function of T/T_c at fixed $\tilde{\mu}_q$.

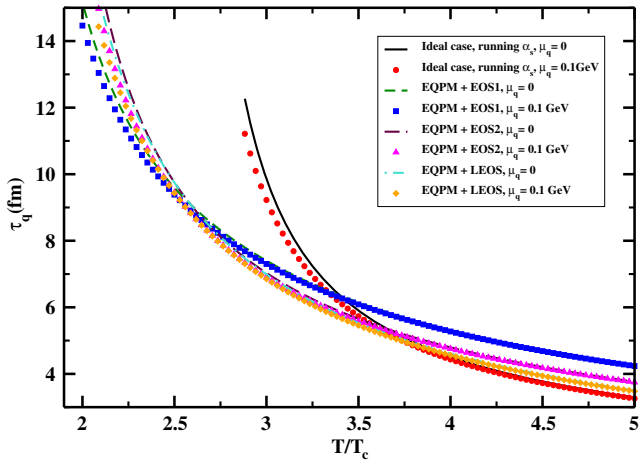

FIG. 3. Thermal relaxation times for quarks using various EOSs as a function of T/T_c at fixed $\tilde{\mu}_q$.

In the present case, τ_g and τ_q have been estimated for three different EOSs (EOS1, EOS2, LEOS) within the scope of EQPM along with ideal EOS with running coupling, and also for two different quark chemical potentials ($\mu_q = 0,\ 0.1$ GeV). As noticed earlier in the case of QCD coupling, here also the finite quark chemical potential effects are only significant at lower temperatures, which diminishes at higher-temperature regions. The large values of τ_g and τ_q for the ideal case at lower temperature mostly result from the higher values of running $\alpha_s(T,\mu_q)(\sim 0.4)$ compared to $\alpha_{\rm eff}(T,\mu_q)(\sim 0.3)$ contributing through the logarithmic term. However, at higher temperatures, the plots of τ's including the quasi-particle equation-of-state effects are merging with the ideal ones, as at those temperature regions, the quasi-particle properties behave almost like those of the free particles. Three different set of plots with EQPM calculations are clearly showing the distinct effects of separate EOSs. In each set, the small but finite effects of nonzero μ_q are observed at lower temperatures, which is more predominant in the plots of τ_q for obvious reasons. So, we conclude first that the logarithmic term in Eq. (23) is playing here the key role in determining the temperature behavior of τ's, and second that different EOSs are describing the interacting medium through various models (pQCD or lattice) and the nonzero μ_q is providing considerable effects on it.

C. Estimation of transport coefficients in the Chapman-Enskog method

The basic scheme of determining the transport coefficients of a many-particle system resides in comparing the macroscopic and microscopic definitions of thermodynamic flows. The description of irreversible phenomena taking place in nonequilibrium systems is characterized by two kinds of concepts: thermodynamic forces and thermodynamic flows. The former create spatial non-uniformities of the macroscopic thermodynamic state variables, while the latter tend to restore the equilibrium situation by wiping out these non-uniformities. Phenomenologically, one finds to within a good approximation that these fluxes are linearly related to the thermodynamic forces where the proportionality constants are termed as transport coefficients. As a consequence, the irreversible part of the energy-momentum tensor and the heat flow can be expressed in a linear law, directly proportional to the corresponding thermodynamic forces, which are, respectively, the velocity gradient and the temperature gradient of the system. From the second law of thermodynamics, it is known that the restoration of equilibrium is achieved by processes which involve increasing entropy. From these criteria, the viscous pressure tensor and the irreversible heat flow of the system are expressed by the equations [89,90]

$$\Pi^{\mu\nu} = 2\eta\langle\partial^\mu u^\nu\rangle + \zeta\Delta^{\mu\nu}\partial\cdot u, \tag{24}$$

$$I^\mu = \lambda(\partial_\sigma T - TDu_\sigma)\Delta^{\mu\sigma}, \tag{25}$$

respectively, where the constants of proportionality η, ζ, and λ are referred to as the transport coefficients. The notation used is explained below. The hydrodynamic velocity u^μ is defined in a comoving frame as $u^\mu = (1,0,0,0)$. $\Delta^{\mu\nu} = g^{\mu\nu} - u^\mu u^\nu$ is the projection operator, with $g^{\mu\nu} = (1,-1,-1,-1)$ as the metric of the system. $\langle t^{\mu\nu}\rangle \equiv [\frac{1}{2}(\Delta^{\mu\alpha}\Delta^{\nu\beta} + \Delta^{\nu\alpha}\Delta^{\mu\beta}) - \frac{1}{3}\Delta^{\mu\nu}\Delta^{\alpha\beta}]t_{\alpha\beta}$ indicates a spacelike symmetric and traceless form of the tensor $t^{\mu\nu}$.

The alternative definition of thermodynamic fluxes at the microscopic level involves an integral over the product of the nonequilibrium or collisional part of the distribution function of particles and an irreducible tensor of the quantity which is being transported. Following this prescription, the viscous pressure tensor and the irreversible heat flow can be given by the following integral equations:

$$\Pi^{\mu\nu} = \sum_{k=1}^{N}\nu_k\int\frac{d^3\vec{p}_k}{(2\pi)^3 p_k^0}\Delta^\mu_\sigma\Delta^\nu_\tau p_k^\sigma p_k^\tau\delta f_k, \tag{26}$$

$$I^\mu = \sum_{k=1}^{N}\nu_k\int\frac{d^3\vec{p}_k}{(2\pi)^3 p_k^0}(p_k.u - h_k)p_k^\sigma\Delta^\mu_\sigma\delta f_k. \tag{27}$$

Here p_k and h_k are the particle four-momenta and enthalpy per particle, respectively. So, comparing the sets of equations in (24), (25) and (26), (27), the values of η, ζ, and λ can be estimated as a function of the particle distribution deviation δf_k.

The fixing of temperature and chemical potential in nonequilibrium systems is essentially done by satisfying the Landau-Lifshitz (LL) conditions. The temperature of the system is fixed by demanding that the energy density in the nonequilibrium case in the LRF be the same as that for the equilibrium case. Similarly, the chemical potential is

fixed by demanding that the number density in the nonequilibrium case, again in the LRF, be the same as that for the equilibrium system. In other words, the shift in energy and number density due to the nonequilibrium terms vanishes at the LRF. In an arbitrary frame, this could be achieved by choosing nonequilibrium terms orthogonal to u^μ. The LL conditions in an arbitrary frame can be written as $u_\mu \delta T^{\mu\nu} u_\nu \equiv 0$ and $u_\mu \delta N^\mu \equiv 0$ (here $\delta T^{\mu\nu}$ is the nonequilibrium decomposition of $T^{\mu\nu}$ and δN^μ is the same for the number current). These conditions are well satisfied in our formalism that is ensured by the form of the nonequilibrium terms. In the context of viscosities within EQPM, the LL conditions are discussed in Ref. [42].

For a system with electrically charged constituents, under the influence of an external electric field, the induced current density relates with the field itself by a linear relation via electrical conductivity (σ_{el}) as

$$J^\mu = \sigma_{el} E^\mu. \tag{28}$$

In a microscopic definition, the current density of such a system is given by

$$J^\mu(x) = \sum_{k=1}^{N} q_k I_k^\mu = \sum_{k=1}^{N-1} (q_k - q_N) I_k^\mu, \tag{29}$$

where q_k is the electric charge associated with the kth species. The diffusion flow I_a^μ for a nonequilibrium relativistic system taking all reactive processes into account is given by

$$I_a^\mu = \sum_{k=1}^{N} q_{ak} I_k, \qquad [a = 1, 2, \ldots N'] \tag{30}$$

$$= \sum_{k=1}^{N} q_{ak} \{N_k^\mu - x_k N^\mu\}. \tag{31}$$

Here a stands for the index of the conserved quantum number, and q_{ak} is the ath conserved quantum number associated with the kth component. $N_k^\mu(x) = \sum_{k=1}^{N} N_k^\mu(x)$ stands for the total particle four-flow, where the particle four-flow for the kth species in a multicomponent system is defined as $N_k^\mu(x) = \int \frac{d^3\vec{p_k}}{(2\pi)^3 p_k^0} p_k^\mu f_k(x, p_k)$. $x_k = \frac{n_k}{n}$ is defined as the particle fraction corresponding to the kth species, with $n_k = \int \frac{d^3\vec{p_k}}{(2\pi)^3} f_k(x, p_k)$ and $n = \sum_{k=1}^{N} n_k(x)$ as the particle number density of the kth species and the total number density of the system, respectively.

Putting Eq. (31) into Eq. (29) and comparing with Eq. (28), we can obtain σ_{el} again as a function of the particle distribution deviation δf_k.

Observing that the transport coefficients depend upon $\delta f_k = f_k^0(1 \pm f_k^0)\phi_k$, we need to obtain a scheme to determine this quantity in an out-of-equilibrium thermodynamic system. We proceed by solving the relativistic transport equation (10) in a technique called the Chapman-Enskog method from the kinetic theory of a multicomponent, many-particle system. In the Chapman-Enskog method, the distribution function is expanded in a series in terms of a parameter. This parameter must be a small, dimensionless quantity in order to make the series asymptotic, such that leading-order terms in the expansion must be significant as compared to the next-to-leading-order ones.

In the presence of an external electromagnetic force, the left-hand side of the relativistic transport equation includes also a covariant force term $q_k F^{\alpha\beta} p_\beta \frac{\partial f_k}{\partial p_k^\alpha}$, where q_k is the electronic charge of the kth-species particle and $F^{\mu\nu} = -u^\mu E^\nu + u^\nu E^\mu$ is the electromagnetic field tensor with electric field E^μ, in the absence of any magnetic field in the medium. After incorporating this force term into Eq. (10), we finally obtain the relativistic transport equation:

$$p_k^\mu \partial_\mu f_k + q_k F^{\alpha\beta} p_\beta \frac{\partial f_k}{\partial p_k^\alpha} = \sum_{l=1}^{N} C_{kl}[f_k, f_l], \quad [k = 1, 2, \ldots N], \tag{32}$$

which, following the Chapman-Enskog hierarchy, finally reduces to the linearized transport equation,

$$p_k^\mu u_\mu (Df_k)^0 + p_k^\mu \nabla_\mu f_k^0 + \frac{1}{T} f_k^0 (1 \pm f_k^0) q_k E_\mu p_k^\mu = -\frac{\omega_k}{\tau_k} f_k^0 (1 \pm f_k^0) \phi_k, \tag{33}$$

with

$$(Df_k)^0 = \frac{\partial f_k^0}{\partial T} DT + \frac{\partial f_k^0}{\partial (\frac{\mu_k}{T})} D\left(\frac{\mu_k}{T}\right) + \frac{\partial f_k^0}{\partial u^\mu} Du^\mu. \tag{34}$$

The terms containing derivatives over $\frac{\mu_k}{T}$ and u^μ follow the conventional prescriptions, while the term having a derivative over temperature picks up the additional part from the energy dispersion relation [Eq. (2)] to produce the correct expression of quasi-particle energy in the linearized transport equation—namely,

$$\frac{\partial f_k^0}{\partial T} = \frac{1}{T^2} f_k^0 (1 \pm f_k^0) \{E_p + T^2 \partial_T ln z_{g/q}\} = \frac{1}{T^2} f_k^0 (1 \pm f_k^0) \omega_k. \tag{35}$$

Following the same treatment for the gradient term of Eq. (33) as well, we finally reduce the transport equation into the following form:

$$f_k^0(1\pm f_k^0)\left[\left\{\frac{\omega_k^2}{T^2}DT+\omega_k D\left\{\frac{\mu_k}{T}\right\}-\omega_k\frac{p_k^\mu}{T}Du^\mu\right\}+\left\{p_k^\mu\frac{\omega_k}{T^2}\nabla_\mu T+p_k^\mu\nabla_\mu\left(\frac{\mu_k}{T}\right)-\frac{p_k^\mu p_k^\nu}{T}\nabla_\mu u_\nu\right\}+\left\{\frac{q_k}{T}E\cdot p_k\right\}\right]=-\frac{\omega_k}{\tau_k}f_k^0(1\pm f_k^0)\phi_k. \tag{36}$$

So, applying the definition of the equilibration momentum distribution function of quasi–quarks/antiquarks and quasi-gluons from Eq. (1) to the left-hand side of Eq. (33), we find a number of terms containing time derivatives and spatial gradients over thermodynamic variables, displayed in Eq. (36). While spatial gradient terms contribute to the thermodynamic forces the time derivatives are needed to be eliminated exploiting a number of thermodynamic identities that are nothing but equilibrium thermodynamic evolution equations of macroscopic state variables of the system, following from certain conservation laws. Hence, we are listing here the evolution equation of the particle number density, the equation of energy evolution, and the equation of motion as follows:

$$Dn_k=-n_k\partial\cdot u, \tag{37}$$

$$\sum_{k=1}^{N}x_k D\omega_k=-\frac{\sum_{k=1}^{N}P_k}{\sum_{k=1}^{N}n_k}\partial\cdot u, \tag{38}$$

$$Du^\mu=\frac{\nabla^\mu P}{\sum_{k=1}^{N}n_k h_k}+\frac{\sum_{k=1}^{N}q_k n_k}{\sum_{k=1}^{N}h_k n_k}E^\mu, \tag{39}$$

with P_k as the partial pressure and $h_k=e_k+\frac{P_k}{n_k}$ as the enthalpy per particle assigned for the kth species. Equation (39) reveals that even if the pressure gradient is zero, the Lorentz force acting on the particles due to the electric field E^μ produces nonzero acceleration.

Replacing the time derivatives with the above mentioned identities, we are left with a number of thermodynamic forces with different tensorial ranks:

$$Q_k X-\langle p_k^\mu p_k^\nu\rangle\langle X_{\mu\nu}\rangle+\langle p_k^\nu\rangle\{(p_k.u)-h_k\}X_{qk}+\langle p_k^\nu\rangle\sum_{a=1}^{N'-1}(q_{ak}-x_a)X_{a\nu}=-\frac{T\omega_k}{\tau_k}\phi_k, \tag{40}$$

with

$$X=\partial\cdot u, \tag{41}$$

$$X_{q\mu}=\left[\frac{\partial_\mu T}{T}-\frac{\partial_\mu P}{nh}\right]+\left[-\frac{1}{h}\sum_{k=1}^{N}x_k q_k E_\mu\right], \tag{42}$$

$$X_{k\mu}=\left[(\partial_\mu\mu_k)_{P,T}-\frac{h_k}{nh}\partial_\mu P\right]\left[q_k-q_N-\frac{h_k-h_N}{h}\sum_{l=1}^{N}x_l q_l\right]E_\mu, \tag{43}$$

$$\langle X_{\mu\nu}\rangle=\langle\partial_\mu u_\nu\rangle=\frac{1}{2}\left\{\Delta_{\mu\alpha}\Delta_{\nu\beta}+\Delta_{\nu\alpha}\Delta_{\mu\beta}-\frac{2}{3}\Delta_{\mu\nu}\Delta_{\alpha\beta}\right\}\partial^\alpha u^\beta. \tag{44}$$

Here, $Q_k=\frac{1}{3}\{|\vec{p_k}|^2-3\omega_k^2c_s^2\}$, where c_s is the velocity of sound propagation within the medium, and $(\partial_\mu\mu_a)_{P,T}=\sum_{b=1}^{N'-1}\{\frac{\partial\mu_a}{\partial x_b}\}_{P,T,\{x_a\}}\partial_\mu x_b$, where x_a and μ_a are the particle fraction and chemical potential associated with the ath quantum number, respectively. Tensors of the forms $\langle p_k^\mu p_k^\nu\rangle=\frac{1}{2}\{\Delta^{\mu\alpha}\Delta^{\nu\beta}+\Delta^{\nu\alpha}\Delta^{\mu\beta}-\frac{2}{3}\Delta^{\mu\nu}\Delta^{\alpha\beta}\}(p_k)_\alpha(p_k)_\beta$ and $\langle p_k^\mu\rangle=\Delta^{\mu\nu}(p_k)_\nu$ are called irreducible tensors of rank 2 and 1, respectively, where the rank 0 is simply a scalar.

Now, we observe that different thermodynamic forces indicated by Eqs. (41)–(44) involve different transport processes. X, expressing the trace part of the velocity gradient, is known as the bulk viscous force. The quantity $X_{q\mu}$ is related to the temperature gradient known as the thermal driving force. $X_{k\mu}$ includes the spatial gradient over chemical potential that can be translated into the gradient over particle fraction $[(\nabla^\mu\mu_k)_{P,T}=\frac{T}{x_k}\nabla^\mu x_k]$, and thus known as the diffusion driving force. Finally, $\langle X_{\mu\nu}\rangle$, containing the traceless part of the velocity gradient is known as the shear viscous force. The respective viscous forces give rise to the shear (η) and bulk (ζ) viscous coefficients, whereas the thermal driving force gives rise to the thermal conductivity λ. We notice that, apart from the spatial gradients over thermodynamic quantities, the thermal driving force and the diffusion driving forces include finite contributions purely from E^μ, reflecting the response of the external electric field in the medium. So we can conclude that in the expressions of thermal and diffusion driving forces, terms proportional to the electric field give rise to electrical conductivity (σ_{el}).

Now, in order to be a solution of Eq. (40), the deviation function ϕ_k must be a linear combination of the thermodynamic forces in the following manner:

$$\phi_k=A_k X+B_k^\mu X_{q\mu}+\frac{1}{T}\sum_{a=1}^{N'-1}B_{ak}^\mu X_{a\mu}-C_k^{\mu\nu}\langle X_{\mu\nu}\rangle, \tag{45}$$

where A, B, and C are the unknown coefficients with appropriate tensorial ranks consistent with the thermodynamic forces, such that ϕ_k becomes a scalar, needed to be estimated from the transport equation itself. In order to do so, we put Eq. (45) on the right-hand side of Eq. (40), and by virtue of the fact that thermodynamic forces are independent of each other, we finally obtain

$$A_k = \frac{Q_k}{\left\{-\frac{T\omega_k}{\tau_k}\right\}}, \qquad B_k^{\mu} = \langle p_k^{\mu}\rangle \frac{\omega_k - h_k}{\left\{-\frac{T\omega_k}{\tau_k}\right\}},$$
$$B_{ak}^{\mu} = T\langle p_k^{\mu}\rangle \frac{q_{ak} - x_a}{\left\{-\frac{T\omega_k}{\tau_k}\right\}}, \qquad C_k^{\mu\nu} = \frac{\langle p_k^{\mu} p_k^{\nu}\rangle}{\left\{-\frac{T\omega_k}{\tau_k}\right\}}. \quad (46)$$

Utilizing the expressions from Eq. (46) and putting them into the expression of ϕ_k from Eq. (45), we finally obtain the full expression of the deviation of the partonic distribution function δf_k. Now we are in a situation where by putting the expression of deviation of the distribution function into the microscopic definitions of thermodynamic fluxes and comparing them with the macroscopic definitions of the same, the transport coefficients can be estimated explicitly, as has been done in the next section.

III. TRANSPORT COEFFICIENTS AND THEIR TEMPERATURE DEPENDENCES

A. Shear viscosity

As discussed in the previous section, in order to estimate the viscous coefficients, we need to compare the expressions of the viscous pressure tensor from Eqs. (24) and (26). It is convenient to split $\Pi^{\mu\nu}$ into a traceless part and a remainder, such as

$$\Pi^{\mu\nu} = \langle \Pi^{\mu\nu}\rangle + \Pi\Delta^{\mu\nu}. \quad (47)$$

The viscous pressure Π is defined as one third of the trace of the viscous pressure tensor,

$$\Pi = \sum_{k=1}^{N} \nu_k \frac{1}{3}\int \frac{d^3\vec{p}_k}{(2\pi)^3 p_k^0}\Delta_{\mu\nu} p_k^{\mu} p_k^{\nu}\delta f_k. \quad (48)$$

So, the traceless part of the viscous pressure tensor comes out to be

$$\langle \Pi^{\mu\nu}\rangle = \Pi^{\mu\nu} - \Pi\Delta^{\mu\nu} = \sum_{k=1}^{N}\nu_k \int \frac{d^3\vec{p}}{(2\pi)^3 p^0}\langle p^{\mu} p^{\nu}\rangle \delta f_k. \quad (49)$$

Clearly, Eq. (48) will give rise to bulk viscosity, while Eq. (49) gives rise to shear viscosity. Putting the expression of δf_k, with the expression of ϕ_k from Eq. (45), into Eq. (49) and comparing with Eq. (24), we can obtain the expression of shear viscosity. In the context of the current article, the shear viscosity for a strongly interacting QGP system is provided with the help of the thermal relaxation times of constituent partons from Eqs. (19) and (20), and the quasi-particle equilibrium distribution functions of the same under the EQPM scheme from Eq. (1) as the following:

$$\eta = \sum_{k=g,q,\bar{q}} \nu_k \frac{\tau_k}{15T}\int \frac{d^3\vec{p}_k}{(2\pi)^3}\frac{|\vec{p_k}|^4}{\omega_k^2} f_k^0(1 \pm f_k^0). \quad (50)$$

Here, the quasi-particle energy per parton under the EQPM model can be derived from the dispersion relation given in Eq. (2) as

$$\omega_k = |\vec{p_k}|\left[1 + \left\{\frac{T}{|\vec{p_k}|}\right\}\left\{\frac{T}{T_c}\right\}\partial_{(\frac{T}{T_c})}\{lnz_k\}\right]. \quad (51)$$

We have estimated η from Eq. (50) in two ways. First, an exact estimation of η from Eq. (50) has been obtained using full numerical coding. Second, we perform an analytical approximation of Eq. (50) in the following manner by investigating its level of accuracy. By analyzing the temperature dependence of the effective fugacity parameter z_k, we have examined the second term on the right-hand side of Eq. (51). For the gluonic case, at $T/T_c = 2.5$ we obtain from Eq. (51) $\omega_g = |\vec{p_g}|[1 + 0.094]$, so the correction in ω_k due to the fugacity term is less than 10%. (Similar estimations can be shown for quark degrees of freedom as well.) So, ω_k can be conveniently expanded in a binomial series keeping only up to second-order terms. Following this prescription, the expression of η, with the analytical approximation performed, becomes

$$\eta = \sum_{k=q,\bar{q},g}\nu_k\frac{\tau_k}{15T}\left[\int\frac{d^3\vec{p}_k}{(2\pi)^3}|\vec{p_k}|^2 f_k^0(1\pm f_k^0) - 2\left\{T\left(\frac{T}{T_c}\right)\partial_{(\frac{T}{T_c})}(lnz_k)\right\}\int\frac{d^3\vec{p}_k}{(2\pi)^3}|\vec{p_k}|f_k^0(1\pm f_k^0)\right]. \quad (52)$$

The full analytic computations of the momentum integrations over the equilibrium quasi-particle distribution functions that give compact results in terms of PolyLog functions of the fugacity parameters of quasi-quarks and gluons are provided in the Appendix.

In Figs. 4 and 5, the obtained shear viscosity over entropy density ratio has been plotted as a function of T/T_c. Figure 4 is showing a comparison between the fully numerical estimation directly from Eq. (50) and the approximated analytical estimation from Eq. (B1) of η/s for $N_f = 3$, with LEOS under the EQPM scheme at $\mu_q = 0.1$ GeV. The plot shows that the two curves are merely separable from each other above $T/T_c \sim 2(T \sim 300$ MeV). So, it can be clearly inferred that the analytical approximation performed in the estimation of η is quite reliable in the temperature range we are interested in currently. Figure 5 exhibits the temperature dependence of η/s estimated under the EQPM scheme using three separate EOSs mentioned in Sec. II A for zero and nonzero μ_q. As predicted by other pQCD estimates, the value of η/s, which is ~0.1, is observed to be greater than the experimental extractions and AdS/CFT predictions. Here the

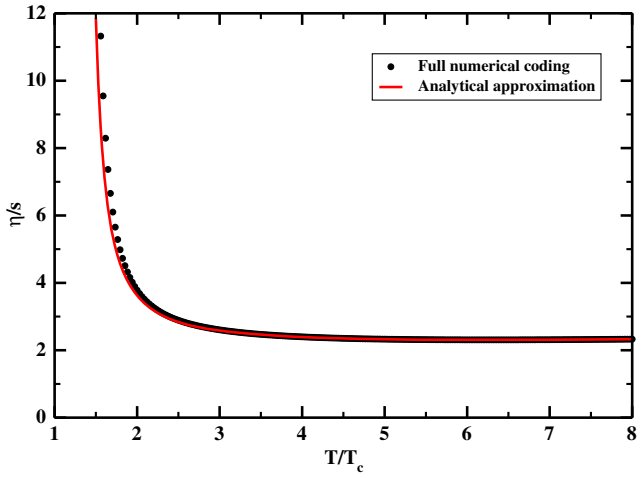

FIG. 4. Comparison between analytical and numerical estimations of the shear viscosity to entropy ratio.

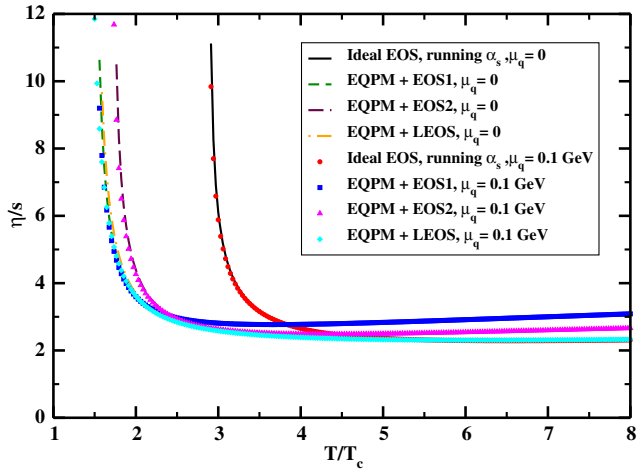

FIG. 5. Shear viscosity to entropy ratio using various EOSs as a function of T/T_c at fixed $\tilde{\mu}_q$.

leading log terms in thermal relaxation time are majorly responsible for the enhanced value of η/s. Up to $T/T_c \sim 4$, the equation-of-state effects under EQPM are quite distinctly visible, while merging with the ideal ones in high-temperature ranges. The nonzero μ_q effects are only slightly visible in lower temperatures, becoming negligible in high temperatures.

B. Bulk viscosity

The bulk viscous coefficients can be estimated in the same spirit as η by comparing Eqs. (48) and (24), and putting the expression of ϕ_k from Eq. (45) into δf_k:

$$\zeta = \sum_{k=q,\bar{q},g} \nu_k \frac{\tau_k}{9T} \int \frac{d^3\vec{p}_k}{(2\pi)^3} \frac{1}{\omega_k^2} \{p_k^2 - 3\omega_k^2 c_s^2\}^2 f_k^0(1 \pm f_k^0). \tag{53}$$

Under the analytical approximation mentioned in the earlier section, Eq. (53) becomes

$$\begin{aligned}\zeta = {} & (1-3c_s^2)^2 \sum_{k=q,\bar{q},g} \nu_k \frac{\tau_k}{9T} \int \frac{d^3\vec{p}_k}{(2\pi)^3} |\vec{p_k}|^2 f_k^0(1 \pm f_k^0) \\ & - 2(1-9c_s^4) \sum_{k=q,\bar{q},g} \nu_k \frac{\tau_k}{9T} \left\{ T\left(\frac{T}{T_c}\right) \partial_{(\frac{T}{T_c})} \{lnz_k\} \right\} \\ & \times \int \frac{d^3\vec{p}_k}{(2\pi)^3} |\vec{p_k}| f_k^0(1 \pm f_k^0) + (1+3c_s^2)^2 \\ & \times \sum_{k=q,\bar{q},g} \nu_k \frac{\tau_k}{9T} \left\{ T\left(\frac{T}{T_c}\right) \partial_{(\frac{T}{T_c})} \{lnz_k\} \right\}^2 \\ & \times \int \frac{d^3\vec{p}_k}{(2\pi)^3} f_k^0(1 \pm f_k^0). \end{aligned} \tag{54}$$

After performing the momentum integrals over separate partonic degrees of freedom, the consolidated expression of ζ in terms of the PolyLog functions over fugacity parameters is given in the Appendix.

In Figs. 6 and 7, the temperature dependence of the estimated ζ/s has been depicted. The former figure again proves the authenticity of the analytical approximation in Eq. (B2), as it agrees sensibly with the full numerical coding [Eq. (54)]. The temperature dependence of ζ/s is displaying the conventional decreasing trend with increasing temperature above T_c, and away from $(T/T_c \sim 2)$ its magnitude appears to be quite small as expected, indicating the diverging nature of ζ only around T_c. We note from Eq. (53) that the ideal EOS will result in a vanishing contribution to ζ for massless QGP. The different EOSs under EQPM are showing distinct temperature behavior of ζ/s around $T/T_c \sim 2$, which are merging together into extremely small values at higher temperatures. However, due to the small order of magnitude of ζ even around T_c (in

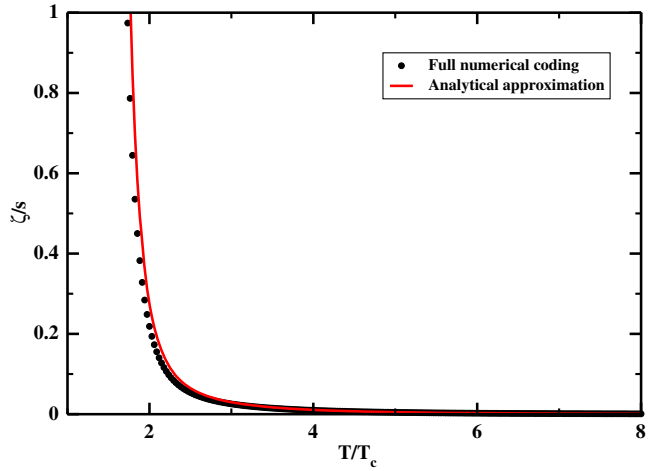

FIG. 6. Comparison between analytical and numerical estimations of the bulk viscosity to entropy ratio.

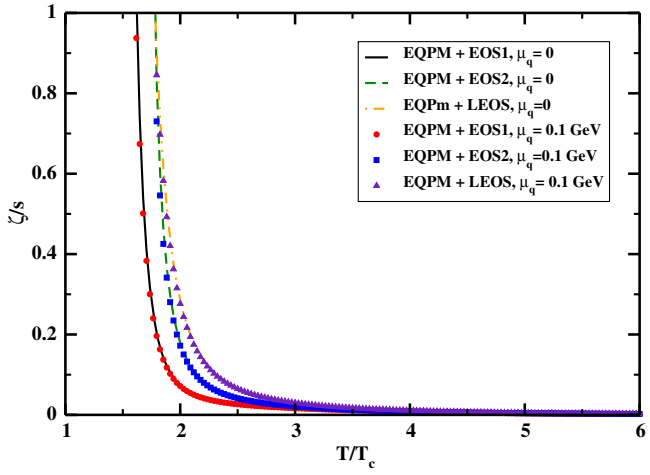

FIG. 7. Bulk viscosity to entropy ratio using various EOSs as a function of T/T_c at fixed $\tilde{\mu}_q$.

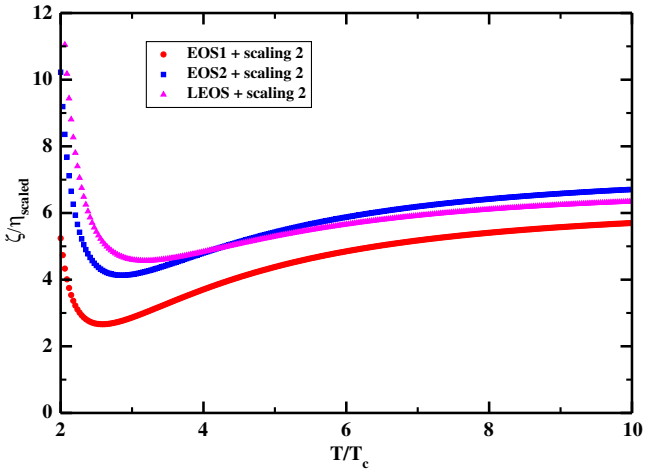

FIG. 9. Bulk viscosity to shear viscosity ratio using scaling 2.

comparison with other transport coefficients), the nonzero quark chemical potential effects are barely visible in this case.

After obtaining the expressions of η and ζ, their ratios have been plotted while scaled with $\{2(1/3 - c_s^2)\}$ (scaling 1) and $\{15(1/3 - c_s^2)^2\}$ (scaling 2), including three different EOS effects and with $\mu_q = 0.1$ GeV in Figs. 8 and 9. These scaling factors have been widely used to illustrate the interplay between bulk and shear viscous coefficients in literature based on pQCD, AdS/CFT, and experimental extractions of transport parameters. However, in our case, the second case offers a better scaling, at least at higher-temperature regions, for all three EOSs, whereas the first one fails to prove a sensible scaling of the ζ/η ratio.

C. Thermal conductivity

The analytical expression of thermal conductivity can be obtained by comparing Eqs. (25) and (27), and replacing ϕ_k in δf_k from Eq. (45) in the following form:

$$\lambda = \sum_{k=q,\bar{q},g} \nu_k \frac{\tau_k}{3T^2} \int \frac{d^3\vec{p}_k}{(2\pi)^3} \frac{|\vec{p_k}|^2}{\omega_k^2} (\omega_k - h_k)^2 f_k^0 (1 \pm f_k^0). \tag{55}$$

An analytical approximation of λ estimated in a similar manner is given in the Appendix.

The results of thermal conductivity are displayed as a function of temperature in Figs. 10 and 11. Like in the other two previous cases, here too the analytical approximation works wonderfully well, showing convincing agreement with full numerical coding. We have plotted the dimensionless quantity λ/T^2 as a function of T/T_c in the second plot, for all possible EOSs and both zero and nonzero quark chemical potentials. As before, the different EOSs are providing recognizably different effects at lower temperatures, which are fusing with the ideal one at higher temperatures. The nonzero μ_q effects are only visible at quite low temperatures. Around $T/T_c \sim 2$, the LEOS

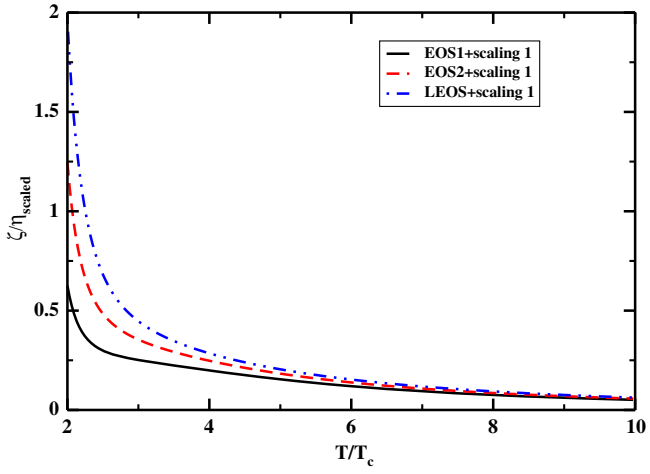

FIG. 8. Bulk viscosity to shear viscosity ratio using scaling 1.

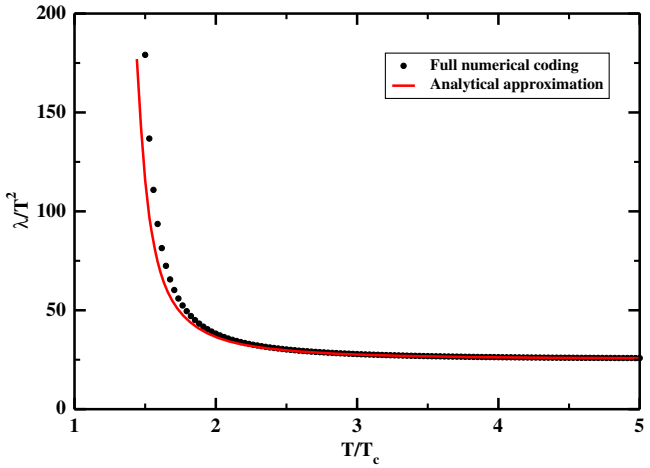

FIG. 10. Comparison between analytical and numerical estimations of thermal conductivity.

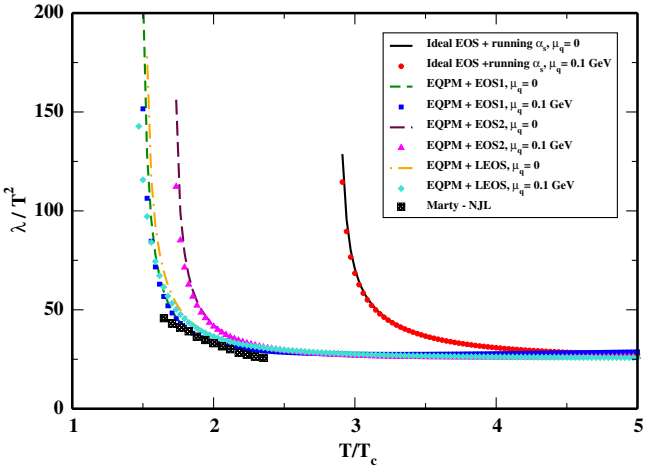

FIG. 11. Thermal conductivity using various EOSs as a function of T/T_c.

results with $\mu_q = 0.1$ GeV are in good agreement with the NJL estimation of thermal conductivity by Marty [49].

D. Electrical conductivity

In order to estimate σ_{el}, we start with the expression of diffusion flow given in Eq. (31). We clearly observe that at leading order with the equilibrium distribution function f_k^0 in the definitions of N_k^μ, N^μ, and x_k, the diffusion flow vanishes, while in the next-to-leading order the correction term $\delta f_k = f_k^0(1 \pm f_k^0)$ gives finite contribution to the diffusion flow as follows:

$$I_a^\mu = \sum_{k=1}^{N}(q_{ak} - x_a) \int \frac{d^3\vec{p}_k}{(2\pi)^3 p_k^0} p_k^\mu f_k^0(1 \pm f_k^0)\phi_k. \quad (56)$$

Using the value of ϕ_k from (45), we get the linear law obeyed by the diffusion flow,

$$I_a^\mu = l_{aq} X_q^\mu + \sum_{b=1}^{N'-1} l_{ab} X_b^\mu, \qquad a = 1, \ldots, (N'-1), \quad (57)$$

where the coefficients associated with thermal diffusion and particle concentration diffusion are given as

$$l_{aq} = \sum_{k=1}^{N}(q_{ak} - x_a) \int \frac{d^3\vec{p}_k}{(2\pi)^3} f_k^0(1 \pm f_k^0) \frac{\tau_k}{T} \frac{|\vec{p}_k|^2}{\omega_k^2}(\omega_k - h_k), \quad (58)$$

$$l_{ab} = \sum_{k=1}^{N}(q_{ak} - x_a)(q_{bk} - x_b) \int \frac{d^3\vec{p}_k}{(2\pi)^3} f_k^0(1 \pm f_k^0) \frac{\tau_k}{T} \frac{|\vec{p}_k|^2}{\omega_k^2}, \quad (59)$$

respectively. Substituting the expression of diffusion flow from Eq. (57) into the microscopic definition of current density in Eq. (29), and pertaining to the terms proportional to the electric field only, we finally obtain the expression for the electric current density as

$$J^\mu = \sum_{k=1}^{N-1}(q_k - q_N)\left[\sum_{l=1}^{N-1} l_{kl}\left\{q_l - q_N - \frac{h_l - h_N}{h}\sum_{n=1}^{N} x_n q_n\right\} - \frac{l_{kq}}{h}\sum_{n=1}^{N} x_n q_n\right] E^\mu. \quad (60)$$

Finally, by comparing Eq. (60) with the macroscopic definition of induced current density from Eq. (28), we get the expression for electrical conductivity as the following:

$$\sigma_{el} = \sum_{k=1}^{N-1}(q_k - q_N)\left[\sum_{l=1}^{N-1} l_{kl}\left\{q_l - q_N - \frac{h_l - h_N}{h}\sum_{n=1}^{N} x_n q_n\right\} - \frac{l_{kq}}{h}\sum_{n=1}^{N} x_n q_n\right]. \quad (61)$$

For a QGP system with quarks, antiquarks, and gluons as the degrees of freedom, the expression of σ_{el} turns out to be

$$\sigma_{el} = q_q^2\left[(l_{11} + l_{21})\left\{1 - \frac{h_q - h_g}{h}(x_q + x_{\bar{q}})\right\} + (l_{12} + l_{22})\left\{1 - \frac{h_{\bar{q}} - h_g}{h}(x_q + x_{\bar{q}})\right\} - (l_{1q} + l_{2q})\frac{(x_q + x_{\bar{q}})}{h}\right], \quad (62)$$

The value $q_q^2 = \sum_k \nu_k q_{qk}^2$ is simply the square of the fractional quark charges taking the sum over quark degeneracy. For up, down, and strange quarks, the fractional quark charges are taken to be $2/3$, $-1/3$, and $-1/3$, respectively. Apart from the full numerical coding, we have done the analytical approximation as well in estimating the value of σ_{el}. For this purpose, the two relevant integrals present in Eqs. (58) and (59), indicated by I_1 and I_2 as follows,

$$\{I_1\}_k = \int \frac{d^3\vec{p}_k}{(2\pi)^3} f_k^0(1 \pm f_k^0) \frac{|\vec{p}_k|^2}{\omega_k^2}(\omega_k - h_k), \quad (63)$$

$$\{I_2\}_k = \int \frac{d^3\vec{p}_k}{(2\pi)^3} f_k^0(1 \pm f_k^0) \frac{|\vec{p}_k|^2}{\omega_k^2}, \quad (64)$$

need to be computed analytically as indicated earlier. The estimated values of the integrals for different partonic degrees of freedom in terms of the fugacity parameters and their derivatives are given in the Appendix.

We end this section by giving the results of electrical conductivity in Figs. 13 and 14. Again, the analytical approximation works quite well, as seen from Fig. 12. The

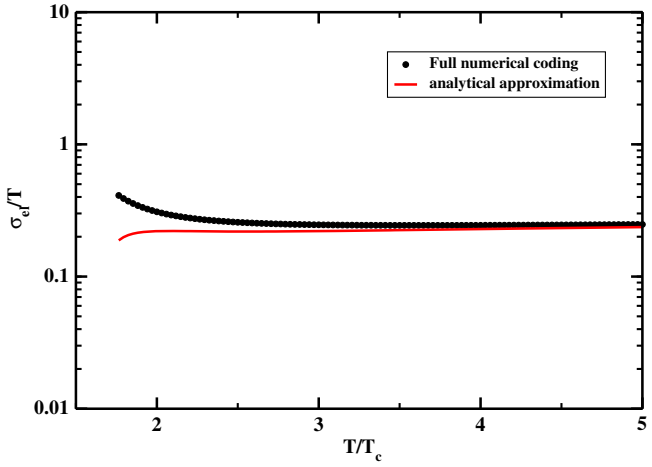

FIG. 12. Comparison between analytical and numerical estimations of σ_{el}.

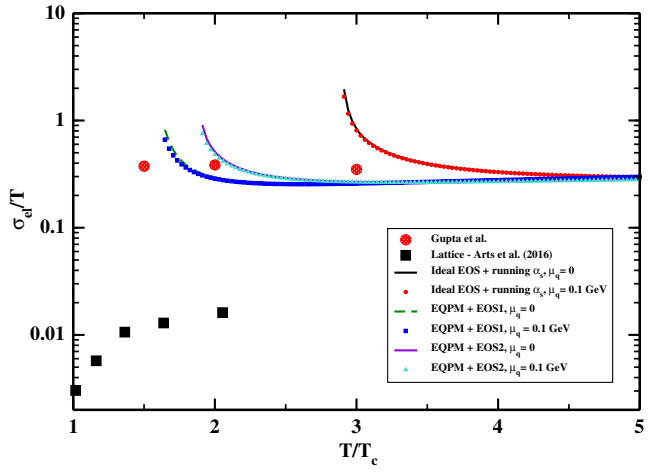

FIG. 13. Electrical conductivity using various EOSs as a function of T/T_c for $N_f = 2$.

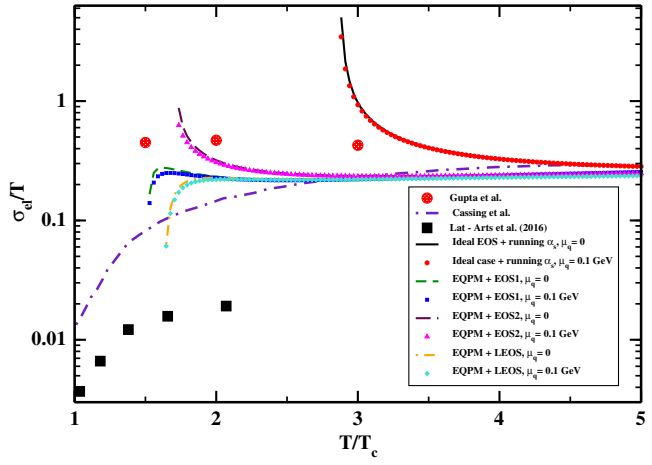

FIG. 14. Electrical conductivity using various EOSs as a function of T/T_c for $N_f = 3$.

dimensionless ratio σ_{el}/T has been plotted against T/T_c for $N_f = 2$ and $N_f = 3$, employing different EOSs in the EQPM. The results with $\mu_q = 0.1$ GeV differ from the same with $\mu_q = 0$ as given in Ref. [57] below $T/T_c \sim 2$, in a small but quantitative amount. The three-flavor case appears to be slightly greater than the two-flavor ones, since the quark charge q_q^2 in Eq. (62) includes the fractional quark charge of the strange quark also. At lower temperatures, the lattice data from Ref. [60] is observed to underpredict the current results; however, the quenched lattice estimations of electrical conductivity from Gupta *et al.* [62] agree with the current estimation of σ_{el} quite sensibly. For the three-flavor case beyond $T/T_c \sim 3$, the estimations of σ_{el} are matching with the trend given in Cassing *et al.* [53] and agree with their statement that above $T \sim 5T_c$, the dimensionless ratio σ_{el}/T becomes approximately constant ($\approx$0.3). In the estimations of σ_{el} throughout, the electronic charges are explicitly given by the relation $\frac{e^2}{4\pi} = \frac{1}{137}$.

E. Relative significance of the transport coefficients and related physical laws

Here, the relative importance of the charge diffusion, the momentum diffusion, and the heat diffusion in a hot QCD medium has been explored by studying the ratios of various transport coefficients, as explicated below.

1. Thermal diffusion vs charge diffusion: The ratio $\lambda/\sigma_{el}T$

The relation between electrical conductivity σ_{el} and thermal conductivity λ for any substance can be understood in terms of the Wiedemann-Franz law. The basic mathematical statement of the law is

$$\frac{\lambda}{\sigma_{el}T} = \mathbf{L}[\mathbf{L}: \text{ Lorenz number}]. \tag{65}$$

For instance, in the case of metals, $\mathbf{L}$ is a constant and quantifies the fact that metals are good electrical as well as thermal conductors. The temperature dependence of the Lorenz number for the QGP/hot QCD is depicted in Fig. 15. For the temperature range $2-10T_c$, $\mathbf{L}$ varies between 250 and 100 for various realistic QGP EOSs. For $T \geq 4T_c$, the number saturates closer to a value 100, which is also the Stefan-Boltzmann (SB) limit (QGP as an ultrarelativistic gas of gluons and quarks). Clearly, the violation is quite apparent for the temperatures which are smaller than $4T_c$ (in fact, the violation becomes quite prominent while moving towards $2T_c$). The law in the case of the QGP mainly depends on the effective coupling, the EOS chosen, and the contributions that are included while computing the thermal relaxation times. To make any sensible argument about the violation and its connection with the other Wiedemann-Franz-law-violating quantum fluids such as

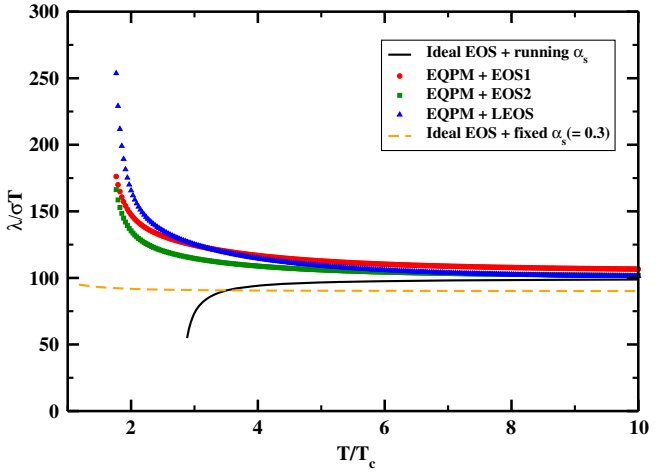

FIG. 15. Lorenz number using various EOSs as a function of T/T_c.

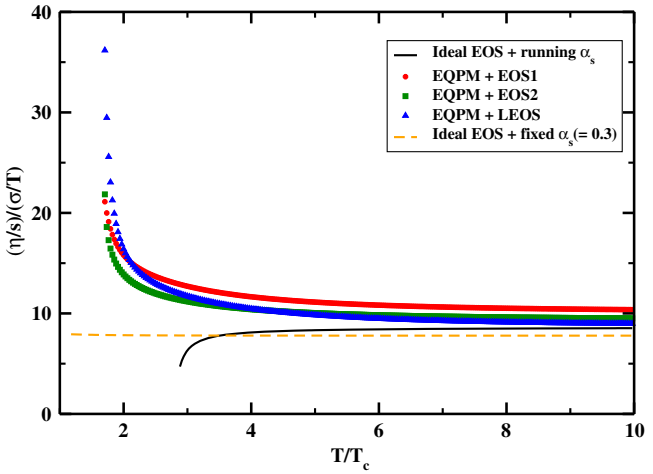

FIG. 16. Shear viscosity to entropy ratio vs electrical conductivity as a function of T/T_c.

graphene [22], a deeper analysis is needed (inclusion of higher-order QCD processes and appropriate collision and source terms in the transport equation and also effects from momentum anisotropy). Nevertheless, the observation from our study perhaps indicates towards a much more complex nature of the QGP as a strongly interacting quantum fluid for temperatures that are not very large compared to the QCD transition temperature, T_c. Noticeably, such deviations have also been observed in holographic anisotropic models that are dual to spatially anisotropic, $\mathcal{N} = 4$ super-Yang-Mills theory at finite chemical potential [91] which further violates the KSS bound of η/S in the longitudinal direction. The numbers obtained in Fig. 15 are slightly higher compared to those from holographic models [24], by holographic estimates.

2. Momentum diffusion vs charge diffusion

The relative significance of the momentum diffusion and the charge diffusion in a medium could be understood in terms of a dimensionless ratio,

$$\mathcal{R}_{\eta/\sigma_{el}} = \frac{\eta/S}{\sigma_{el}/T}. \tag{66}$$

In a hot QCD medium, unlike gluons, a quark (antiquark) carries EM charge. Therefore, it is reasonable to expect that its contribution to the σ_{el} would be predominant, as gluons enter only through the interactions (qg and gg scattering contributions). Since the gluonic scattering rates are larger as compared to that for the quarks and antiquarks, the quark contribution to the shear viscosity is also expected to be dominant. The ratio $\mathcal{R}_{\eta/\sigma_{el}}$ could be an indicator of the relative significance of the gluonic and matter sectors as far as the relative importance of the momentum and the charge transports in the QGP medium are concerned. This point has been realized to some degree of detail in Ref. [27], where a scaling in terms of gluon and quark relaxation times was seen. In contrast, in the present analysis, such a scaling highlighting the relative importance of gluonic and quark contributions is not expected due to the more systematic treatment of the scattering cross sections and the computation of relaxation times and inclusion of all the relevant effects from the gluonic sector. The ratio decreases with increasing temperature and subsequently saturates towards the SB limit (the black line in Fig. 16). The ratio is always greater than unity for the whole range of temperature. It can be inferred that the momentum transfer has dominant impact over the charge diffusion.

3. Momentum diffusion vs thermal diffusion: The Prandtl number for the QGP

The relative magnitude of the momentum and the thermal diffusions is quantified in terms of the Prandtl number, Pr (the ratio of momentum diffusibility and thermal diffusibility):

$$\mathrm{Pr} = \frac{\eta c_p}{\rho\lambda}, \tag{67}$$

where c_p is the specific heat at constant pressure. This number signifies the relative importance of shear viscosity and thermal conductivity in the sound attenuation in a liquid medium. Before describing it for a hot QCD/QGP medium, let us get an idea about its magnitude for other strongly coupled systems. For liquid helium, the Prandtl number is around 2.5 [9]; for a weakly interacting unitary Fermi gas at high temperature, it is $2/3$ [9,92]. On the other hand, for conformal nonrelativistic theories, the number is of the order of 1 [25].

To define the Prandtl number for the QGP, apart from η, σ_{el}, and c_p, one needs to know the mass density ρ. The only mass scale in high-temperature QCD is the thermal mass of

a dressed parton (gluon or quark) that is obtained in terms of the QCD effective coupling constant at high temperature and the temperature scale of the system. In our case, the mass density for the QGP can be defined as

$$\rho = m_g n_g + m_q(n_q + n_{\bar{q}}), \tag{68}$$

where m_g and m_q are the thermal (medium) masses of the gluons and quarks, respectively, and n_g, $n_{q,\bar{q}}$ are their respective number densities obtained from the momentum distributions, following the basic thermodynamic definitions.

The gluon medium mass m_g and quark medium mass m_q for the QCD are obtained in terms of gluon and quark/antiquark distributions functions as [93]

$$\begin{aligned} m_g^2(=m_D^2) &\equiv 4\pi\alpha_s(T,\mu_q)\left\{-2N_c\int\frac{d^3\vec{p}}{(2\pi)^3}\partial_p f_g(\vec{p})\right. \\ &\left. - N_f\int\frac{d^3p}{(2\pi)^3}\partial_p(f_q(\vec{p})+f_{\bar{q}}(\vec{p}))\right\}, \\ m_q^2 &= \left(\frac{N_c^2-1}{2N_c}\right)4\pi\alpha_s(T,\mu_q) \\ &\times\int\frac{d^3\vec{p}}{(2\pi)^3|\vec{p}|}\left\{f_g(\vec{p})+\left(\frac{f_q(\vec{p})+f_{\bar{q}}(\vec{p})}{2}\right)\right\}. \end{aligned} \tag{69}$$

The number is plotted as a function of T/T_c in Fig. 17 for various EOSs within their EQPM descriptions. The number is in the range 20–35 for the all cases considered here. All the other liquids/systems mentioned previously possess much smaller numbers as compared to the QGP; therefore, sound attenuation is mostly governed by the momentum diffusion here. In this context, we may perhaps ignore the effects that are coming from thermal diffusion, unlike holographic models, where both these effects are on an equal footing.

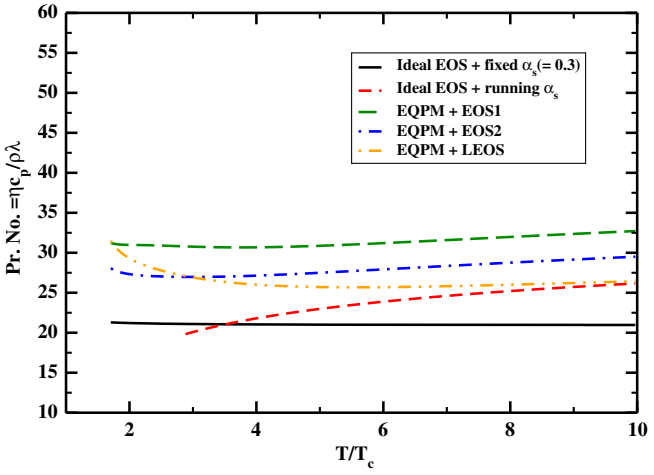

FIG. 17. Prandtl number using various EOSs as a function of T/T_c.

IV. DISCUSSIONS ON THE RESULTS

The present result for η/S based on the EQPM model, employing binary elastic scattering processes among quarks and gluons, turned out to be closer to predictions from pQCD and effective theory-based models [33]. However, a sharp rise of η/S below $T/T_c \sim 3$ indicates the nontrivial α_s dependence of the interaction cross section through the logarithmic behavior. In most of the pQCD estimations, the cross section is proportional to α_s, leading to $\eta/s \sim 1/\alpha_s$ [41]. In the present case, the $\tau^{-1} \sim \alpha_s^2 ln\{\frac{1}{\alpha_s}\}$ term is controlling the behavior of η/S crucially, which leads to the sharp increase of η/S at lower temperatures with $\alpha_s \sim 0.3$–0.4, where the logarithmic term predominates, and the moderate increase at higher temperature with $\alpha_s \sim 0.15$, where the α_s^2 term prevails. Hence, we conclude that the EQPM model—which is basically dressing up the bare particles by defining their collective properties in a thermal medium, and those properties are being reflected through the logarithmic term in the viscosity—is responsible for the large values (∼2) of η/S. In this context, the significance of the inelastic processes will be a matter of future investigations. Our results on bulk viscosity are observed to be consistent with other perturbative estimates on the same. In all the estimations of bulk viscous coefficient, the value of ζ/s has been reported to be extremely smaller except near T_c. In Ref. [44], the 3D hybrid simulation agrees with data from ALICE and CMS for $\zeta/s \approx 0.3$ around T_c. The lattice Monte Carlo calculation for $SU(3)$ gluodynamics in Ref. [14] reports $\zeta/s < 0.15$ near T_c $(T/T_c = 1.65)$, which becomes negligibly small $\zeta/s < 0.015$ away from T_c. The leading-order pQCD estimation from Ref. [94] also gives a small value of bulk viscosity, $\zeta = 0.2\alpha_s^2 T^3$, for reasonable perturbative values of $0.2 \lesssim \alpha_s \lesssim 0.3$.

In comparison to the viscosities, the investigations on thermal conductivity are really quite limited in the existing literature. In Ref. [48], the λ of a massless Boltzmann gas using the partonic cascade model has been listed as a temperature-independent quantity for a number of isotropic cross sections. In Ref. [49], the dimensionless quantity λ/T^2 has been plotted against T/T_c for both the NJL model and the dynamical quasi-particle particle model (DQPM), which displays two completely different trends. However, at lower temperature ranges $(T/T_c \sim 1.5$–$2.5)$, our estimations appear to be quite consistent at the quantitative level with the NJL one. On the other hand, the lattice data from Refs. [59–61,63,64] provide an estimation for σ_{el}/T that is below 0.05, up to temperature 350 MeV, which quite underpredicts our results, but the quenched lattice estimation from Ref. [62] offers quite sensible agreement. The DQPM results from Ref. [53] also exhibit a compatible

trend with our result. The maximum entropy method (MEM) according to Ref. [55] gives $\sigma_{el}/T \sim 0.4$ at $T/T_c = 3$, which is also close to our result.

Interplay of the thermal diffusion and the electrical diffusion could be understood in terms of the Wiedemann-Franz law—the dimensionless number (Lorenz number). For a large class of metals, this is constant and depicts the common origin of both the transport processes. In other words, the metals are good thermal and electrical conductors at the same time. The Lorenz number for the hot QCD system in the current work converges to a number slightly higher than 100 at higher temperatures. For the temperatures that are lower than $3T_c$, there is a significant rise as we decrease the temperature. This indicates towards the violation of the above mentioned law. In some known systems, such as graphene, this violation leads to a strongly interacting quantum fluid also termed as Dirac fluid [22]. In this present case, the violation is mainly due to the $1/\alpha_s$ term and the strongly interacting EOS. To make any such concrete connection with the other interesting quantum fluids is quite early, as it will require more refined computation of the Lorenz number while including higher-order hot QCD effects in the current analysis. This will be one direction on which the future investigation will focus. In order to explore the relative importance of the momentum diffusion and the charge diffusion in the hot QCD medium, the ratio of η/s to σ_{el}/T is studied as a function of temperature. The ratio for the QGP turns out to be much greater than unity for the whole range of the temperature considered here, indicating the more prominent role of the momentum diffusion in agreement with the prediction of Ref. [27]. Finally, the relative significance of the thermal and the momentum diffusions has been quantified in terms of the Prandtl number. For the hot QCD system here, this number came out to be much greater than unity, signifying the dominance of the momentum diffusion over the thermal one. In other words, sound attenuation in the hot QCD/QGP system will mainly be governed by the shear viscous effects, which is in contrast to the observations for dilute Fermi gases [9] or the holographic systems [25]. For example, in liquid helium, the number is 2.5 [9], which is but an order of magnitude smaller.

V. CONCLUSIONS AND OUTLOOK

The current article is concerned with the temperature behavior of various transport coefficients that measure the dissipative and electromagnetic responses in a strongly interacting QCD system at finite temperature with nonzero quark chemical potential. The most important feature of this work is to highlight the concerned physical laws expressing the relative importance of different transport phenomena by obtaining the temperature dependences of their mutual ratios. The detailed Chapman-Enskog technique for a multicomponent fluid, adopted from the kinetic theory of many-particle systems, has been discussed, which gives the mathematical expressions of shear and bulk viscosities, thermal conductivity, and electrical conductivity in terms of the medium interactions. The interaction cross sections are provided through the thermal relaxation times of constituent quarks, antiquarks, and gluons by leading-order QCD estimations. The effects of a strongly coupled thermal medium have been introduced in the evaluation of these transport parameters through the EQPM model, which describes the collective properties of quarks and gluons by considering them as quasi-particles rather than bare ones. The finite-temperature effects have been folded through this EQPM scheme by introducing the pQCD- and lattice-QCD-based equation-of-state effects in particle momentum distribution and effective couplings. Finally, they are applied to the current formalism of estimating transport coefficients and studying the related physical laws. So we conclude by saying that we have investigated the transport properties and electromagnetic responses along with the associated physical laws in a strongly interacting hot QCD medium quite thoroughly and reasonably, presenting a sensible, realistic scenario created out of the relativistic heavy-ion collisions. The results obtained in our approach are seen to be consistent with other parallel or distinct approaches.

The current work opens up a horizon of possible extensions and applications in related areas in the near future—e.g., the inclusion of more realistic collision terms that ensure local number and energy-momentum conservations away from equilibrium (such as BGK [95] and other nonlocal collision terms) along with the Vlasov term to accommodate the influence of color fields in the initial stages of the RHIC, while setting up the transport equation that estimates the transport coefficients will be a significant improvement. The viscosities controlling the magnitude of hydrodynamic fluctuations in the fluid can be extracted directly from the correlation observables in heavy-ion collisions [96]. This can offer a means to predict the viscosity, independent from the traditional collective flow analysis and can shed some light regarding the dissimilarities in the viscosity values extracted by them from the pQCD measurements. Finally, the estimations of all the above mentioned transport coefficients by including higher-order thermal QCD effects with appropriate collision, Vlasov, and source terms in the transport equation while also including the anisotropic aspects of the QGP in heavy-ion collisions could be another interesting direction for future explorations to focus on.

ACKNOWLEDGMENTS

V. C. would like to acknowledge the Department of Science and Technology (DST), Government of India for the INSPIRE Faculty Fellowship (IFA-13/PH-55) and the Science and Engineering Research Board (SERB), DST, for granting funds under the Early Career Research Award

(ECRA). S. M. acknowledges the Indian Institute of Technology Gandhinagar for the Institute Postdoctoral Fellowship.

APPENDIX A: ENERGY-MOMENTUM CONSERVATION IN EFFECTIVE KINETIC THEORY WITH EQPM

The energy-momentum conservation could be realized in terms of the first moment of the transport equation, (32), as

$$\sum_k \int \frac{d^3\vec{p}}{(2\pi)^3\omega_k} p^\nu p^\mu \partial_\mu f_k = \sum_k \int \frac{d^3\vec{p}}{(2\pi)^3\omega_k} p^\nu C[f_k]. \tag{A1}$$

The right-hand side of Eq. (A1) vanishes by virtue of the summation invariant. The left-hand side breaks up into the following two parts:

$$\sum_k \left(\partial_\mu \int \frac{d^3\vec{p}}{(2\pi)^3\omega_k} p^\nu p^\mu f_k - \int \frac{d^3\vec{p}}{(2\pi)^3} \partial_\mu \left(\frac{p^\nu p^\mu}{\omega_k} \right) f_k \right) = 0. \tag{A2}$$

The second term could be neglected, since it involves only second-order derivatives, or products of first-order derivatives or higher-order ones. This can be seen below. Let us define the second term as

$$I = \int \frac{d^3\vec{p}}{(2\pi)^3} \partial_\mu \left(\frac{p^\mu p^\nu}{\omega_k} \right) f_k. \tag{A3}$$

Here, p^μ (in LRF) could be written in terms of bare momentum $p'^\mu \equiv \{E_k, \vec{p}\}$ as $p^\mu = p'^\mu + \Delta u^\mu$, with $\Delta = T^2 \partial_T \ln(z_{g,q})$. Following this definition, Eq. (A3) will lead to

$$\begin{aligned} \partial_\mu \left(\frac{p^\mu p^\nu}{\omega_k} \right) = {} & \frac{2\Delta}{\omega_k} u^\nu D\Delta - \frac{\Delta^2}{\omega_k^2} u^\nu D\Delta + \frac{E_p}{\omega_k^2} p'^\nu D\Delta \\ & + \frac{E_p}{\omega_k^2} u^\nu p'^\mu \partial_\mu \Delta - \frac{1}{\omega_k^2} p'^\mu p'^\nu \partial_\mu \Delta \\ & + \frac{1}{\omega_k} \Delta p'^\mu \partial_\mu u^\nu + \frac{\Delta^2}{\omega_k} D u^\nu \\ & + \frac{1}{\omega_k} \Delta p^\nu \partial \cdot u + \frac{1}{\omega_k} \Delta^2 u^\nu \partial \cdot u, \end{aligned} \tag{A4}$$

where $D = u^\mu \partial_\mu$. As stated earlier, all the terms are either second order in gradients or the product of two first-order derivatives in gradients or higher ones. Therefore, in developing first-order dissipative hydrodynamics, these terms have been neglected. In view of the above considerations, Eq. (A1) can be rewritten as

$$\partial_\mu T^{\mu\nu}_{QP} \equiv 0, \tag{A5}$$

with $T^{\mu\nu}_{QP}$ having the following expression:

$$T^{\mu\nu}_{QP} = \sum_k \int \frac{d^3\vec{p}}{(2\pi)^3\omega_k} p^\nu p^\mu f_k. \tag{A6}$$

APPENDIX B: FULL ANALYTIC EXPRESSION OF TRANSPORT COEFFICIENTS

The analytic expressions for various transport parameters of the QGP and some integrals involved while computing the electrical conductivity σ_{el} are listed below.

The shear viscosity η is obtained as

$$\begin{aligned} \eta = {} & \left(\frac{2T^4}{5\pi^2}\right)\nu_g\tau_g \left[2\text{Polylog}[4, z_g] - \left\{ \left(\frac{T}{T_c}\right) \partial_{(\frac{T}{T_c})} (lnz_g) \right\} \text{Polylog}[3, z_g] \right] + \left(\frac{2T^4}{5\pi^2}\right)\nu_q\tau_q \left[-2 \left\{ \text{Polylog}[4, -z_q] \right.\right. \\ & \left. + \tilde{\mu_q} \text{Polylog}[3, -z_q] + \frac{\tilde{\mu_q}^2}{2} \text{Polylog}[2, -z_q] \right\} + \left\{ \left(\frac{T}{T_c}\right) \partial_{(\frac{T}{T_c})} (lnz_q) \right\} \left\{ \text{Polylog}[3, -z_q] + \tilde{\mu_q} \text{Polylog}[2, -z_q] \right. \\ & \left.\left. - \frac{\tilde{\mu_q}^2}{2} ln(1 + z_q) \right\} \right] + \left(\frac{2T^4}{5\pi^2}\right)\nu_{\bar{q}}\tau_{\bar{q}} \left[-2 \left\{ \text{Polylog}[4, -z_q] - \tilde{\mu_q} \text{Polylog}[3, -z_q] + \frac{\tilde{\mu_q}^2}{2} \text{Polylog}[2, -z_q] \right\} \right. \\ & \left. + \left\{ \left(\frac{T}{T_c}\right) \partial_{(\frac{T}{T_c})} (lnz_q) \right\} \left\{ \text{Polylog}[3, -z_q] - \tilde{\mu_q} \text{Polylog}[2, -z_q] - \frac{\tilde{\mu_q}^2}{2} ln(1 + z_q) \right\} \right]. \end{aligned} \tag{B1}$$

The bulk viscosity ζ is obtained as

$$\zeta = (1-3c_s^2)^2\tau_g\nu_g\left(\frac{4T^4}{3\pi^2}\right)\text{PolyLog}[4,z_g] - (1-9c_s^4)\tau_g\nu_g\left(\frac{2T^4}{3\pi^2}\right)\left[\left(\frac{T}{T_c}\right)\partial_{(\frac{T}{T_c})}(lnz_g)\right]\text{PolyLog}[3,z_g]$$
$$+ (1+3c_s^2)^2\tau_g\nu_g\left(\frac{T^4}{9\pi^2}\right)\left[\left(\frac{T}{T_c}\right)\partial_{(\frac{T}{T_c})}(lnz_g)\right]^2\text{PolyLog}[2,z_g] + (1-3c_s^2)^2\tau_q\nu_q\left(\frac{4T^4}{3\pi^2}\right)\left[-\left\{\text{PolyLog}[4,-z_q]\right.\right.$$
$$\left.+\tilde{\mu_q}\text{Polylog}[3,-z_q] + \frac{\tilde{\mu_q}^2}{2}\text{Polylog}[2,-z_q]\right\}\Big] - (1-9c_s^4)\tau_q\nu_q\left(\frac{2T^4}{3\pi^2}\right)\left[\left(\frac{T}{T_c}\right)\partial_{(\frac{T}{T_c})}(lnz_q)\right]\left[-\left\{\text{PolyLog}[3,-z_q]\right.\right.$$
$$\left.+\tilde{\mu_q}\text{Polylog}[2,-z_q] - \frac{\tilde{\mu_q}^2}{2}ln(1+z_q)\right\}\Big] + (1+3c_s^2)^2\tau_q\nu_q\left(\frac{T^4}{9\pi^2}\right)\left[\left(\frac{T}{T_c}\right)\partial_{(\frac{T}{T_c})}(lnz_q)\right]^2\left[-\left\{\text{PolyLog}[2,-z_q]\right.\right.$$
$$\left.-\tilde{\mu_q}ln(1+z_q) - \frac{\tilde{\mu_q}^2}{2}\frac{z_q}{1+z_q}\right\}\Big] + (1-3c_s^2)^2\tau_{\bar{q}}\nu_{\bar{q}}\left(\frac{4T^4}{3\pi^2}\right)\left[-\left\{\text{PolyLog}[4,-z_q] - \tilde{\mu_q}\text{Polylog}[3,-z_q]\right.\right.$$
$$\left.+\frac{\tilde{\mu_q}^2}{2}\text{Polylog}[2,-z_q]\right\}\Big] - (1-9c_s^4)\tau_{\bar{q}}\nu_{\bar{q}}\left(\frac{2T^4}{3\pi^2}\right)\left[\left(\frac{T}{T_c}\right)\partial_{(\frac{T}{T_c})}(lnz_q)\right]\left[-\left\{\text{PolyLog}[3,-z_q] - \tilde{\mu_q}\text{Polylog}[2,-z_q]\right.\right.$$
$$\left.-\frac{\tilde{\mu_q}^2}{2}ln(1+z_q)\right\}\Big] + (1+3c_s^2)^2\tau_{\bar{q}}\nu_{\bar{q}}\left(\frac{T^4}{9\pi^2}\right)\left[\left(\frac{T}{T_c}\right)\partial_{(\frac{T}{T_c})}(lnz_q)\right]^2\left[-\left\{\text{PolyLog}[2,-z_q] + \tilde{\mu_q}ln(1+z_q) - \frac{\tilde{\mu_q}^2}{2}\frac{z_q}{1+z_q}\right\}\right]. \tag{B2}$$

The thermal conductivity of hot QCD, λ, is obtained as

$$\lambda = \left(\frac{2T^3}{9\pi^2}\right)\nu_g\tau_g\left[2\text{Polylog}[4,z_g] - \left\{\left(\frac{T}{T_c}\right)\partial_{(\frac{T}{T_c})}(lnz_g)\right\}\text{Polylog}[3,z_g]\right]$$
$$+ \left(\frac{2T^3}{9\pi^2}\right)\nu_q\tau_q\left[-2\left\{\text{Polylog}[4,-z_q] + \tilde{\mu_q}\text{Polylog}[3,-z_q] + \frac{\tilde{\mu_q}^2}{2}\text{Polylog}[2,-z_q]\right\} + \left\{\left(\frac{T}{T_c}\right)\partial_{(\frac{T}{T_c})}(lnz_q)\right\}\right.$$
$$\left.\times\left\{\text{Polylog}[3,-z_q] + \tilde{\mu_q}\text{Polylog}[2,-z_q] - \frac{\tilde{\mu_q}^2}{2}ln(1+z_q)\right\}\right] + \left(\frac{2T^3}{9\pi^2}\right)\nu_{\bar{q}}\tau_{\bar{q}}\left[-2\left\{\text{Polylog}[4,-z_q] - \tilde{\mu_q}\text{Polylog}[3,-z_q]\right.\right.$$
$$\left.+\frac{\tilde{\mu_q}^2}{2}\text{Polylog}[2,-z_q]\right\} + \left\{\left(\frac{T}{T_c}\right)\partial_{(\frac{T}{T_c})}(lnz_q)\right\}\left\{\text{Polylog}[3,-z_q] - \tilde{\mu_q}\text{Polylog}[2,-z_q] - \frac{\tilde{\mu_q}^2}{2}ln(1+z_q)\right\}\Big]. \tag{B3}$$

The integral identities that are used in obtaining electrical conductivity σ_{el} are listed below:

$$\{I_1\}_g = -\frac{T^4}{\pi^2}\left[\text{PolyLog}[3,z_g] - \frac{2}{3}\left\{\left(\frac{T}{T_c}\right)\partial_{(\frac{T}{T_c})}(lnz_g)\right\}\text{PolyLog}[2,z_g]\right], \tag{B4}$$

$$\{I_1\}_{q/\bar{q}} = \frac{T^4}{\pi^2}\left[\text{PolyLog}[3,-z_q] \pm \tilde{\mu_q}\text{PolyLog}[2,-z_q] - \frac{\tilde{\mu_q}^2}{2}ln(1+z_q)\right] - \frac{2T^4}{3\pi^2}\left\{\left(\frac{T}{T_c}\right)\partial_{(\frac{T}{T_c})}(lnz_q)\right\}$$
$$\times\left[\text{PolyLog}[2,-z_q] \mp \tilde{\mu_q}ln(1+z_q) - \frac{\tilde{\mu_q}^2}{2}\frac{z_q}{1+z_q}\right], \tag{B5}$$

$$\{I_2\}_g = \frac{T^3}{\pi^2}\text{PolyLog}[2,z_g] + \frac{T^3}{\pi^2}\left\{\left(\frac{T}{T_c}\right)\partial_{(\frac{T}{T_c})}(lnz_g)\right\}ln(1-z_g), \tag{B6}$$

$$\{I_2\}_{q/\bar{q}} = \frac{-T^3}{\pi^2}\left[\text{PolyLog}[2,-z_q] \mp \tilde{\mu_q}ln(1+z_q) - \frac{\tilde{\mu_q}^2}{2}\frac{z_q}{1+z_q}\right] - \frac{T^3}{\pi^2}\left\{\left(\frac{T}{T_c}\right)\partial_{(\frac{T}{T_c})}(lnz_q)\right\}$$
$$\times\left[ln(1+z_q) \pm \tilde{\mu_q}\frac{z_q}{1+z_q} + \frac{\tilde{\mu_q}^2}{2}\frac{z_q}{(1+z_q)^2}\right]. \tag{B7}$$

[1] B. I. Abelev *et al.* (STAR Collaboration), Centrality dependence of charged hadron and strange hadron elliptic flow from $\sqrt{s_{NN}} = 200$ GeV Au + Au collisions, Phys. Rev. C **77**, 054901 (2008).

[2] M. Luzum and P. Romatschke, Conformal relativistic viscous hydrodynamics: Applications to RHIC results at $\sqrt{s_{NN}} = 200$ GeV, Phys. Rev. C **78**, 034915 (2008).

[3] J. Adam *et al.* (ALICE Collaboration), Correlated Event-by-Event Fluctuations of Flow Harmonics in Pb-Pb Collisions at $\sqrt{s_{\rm NN}} = 2.76$ TeV, Phys. Rev. Lett. **117**, 182301 (2016); Anisotropic Flow of Charged Particles in Pb-Pb Collisions at $\sqrt{s_{\rm NN}} = 5.02$ TeV, Phys. Rev. Lett. **116**, 132302 (2016); B. Abelev *et al.* (ALICE Collaboration), Directed Flow of Charged Particles at Midrapidity Relative to the Spectator Plane in Pb-Pb Collisions at $\sqrt{s_{NN}} = 2.76$ TeV, Phys. Rev. Lett. **111**, 232302 (2013); Charge Separation Relative to the Reaction Plane in Pb-Pb Collisions at $\sqrt{s_{NN}} = 2.76$ TeV, Phys. Rev. Lett. **110**, 012301 (2013); J. Adam *et al.* (ALICE Collaboration), Charge-dependent flow and the search for the chiral magnetic wave in Pb-Pb collisions at $\sqrt{s_{\rm NN}} = 2.76$ TeV, Phys. Rev. C **93**, 044903 (2016); Higher harmonic flow coefficients of identified hadrons in Pb-Pb collisions at $\sqrt{s_{\rm NN}} = 2.76$ TeV, J. High Energy Phys. 09 (2016) 164.

[4] Y. Hirono, M. Hongo, and T. Hirano, Estimation of electric conductivity of the quark gluon plasma via asymmetric heavy-ion collisions, Phys. Rev. C **90**, 021903 (2014); U. Gursoy, D. Kharzeev, and K. Rajagopal, Magnetohydrodynamics and charged currents in heavy ion collisions, Nucl. Phys. **A931**, 986 (2014); Magnetohydrodynamics, charged currents, and directed flow in heavy ion collisions, Phys. Rev. C **89**, 054905 (2014); L. McLerran and V. Skokov, Comments about the electromagnetic field in heavy-ion collisions, Nucl. Phys. **A929**, 184 (2014); V. Toneev, O. Rogachevsky, and V. Voronyuk, Evidence for creation of strong electromagnetic fields in relativistic heavy-ion collisions, Eur. Phys. J. A **52**, 264 (2016); V. Voronyuk, V. D. Toneev, S. A. Voloshin, and W. Cassing, Charge-dependent directed flow in asymmetric nuclear collisions, Phys. Rev. C **90**, 064903 (2014); C. H. Lee and I. Zahed, Electromagnetic radiation in hot QCD matter: Rates, electric conductivity, flavor susceptibility and diffusion, Phys. Rev. C **90**, 025204 (2014).

[5] S. Mitra, S. Ghosh, and S. Sarkar, Effect of spectral modification of ρ on shear viscosity of a pion gas, Phys. Rev. C **85**, 064917 (2012); S. Mitra and S. Sarkar, Medium effects on the viscosities of a pion gas, Phys. Rev. D **87**, 094026 (2013); U. Gangopadhyaya, S. Ghosh, S. Sarkar, and S. Mitra, In-medium viscous coefficients of a hot hadronic gas mixture, Phys. Rev. C **94**, 044914 (2016); S. Mitra and S. Sarkar, Medium effects on the thermal conductivity of a hot pion gas, Phys. Rev. D **89**, 054013 (2014).

[6] V. Chandra, R. Kumar, and V. Ravishankar, Hot QCD equation of state and relativistic heavy ion collisions, Phys. Rev. C **76**, 054909 (2007); Publisher's Note, Phys. Rev. C **76**, 069904(E) (2007).

[7] V. Chandra, A. Ranjan, and V. Ravishankar, On the chromoelectric permittivity and Debye screening in hot QCD, Eur. Phys. J. A **40**, 109 (2009).

[8] T. Schaefer, Fluid dynamics and viscosity in strongly correlated fluids, Annu. Rev. Nucl. Part. Sci. **64**, 125 (2014).

[9] T. Schaefer and D. Teaney, Nearly perfect fluidity: From cold atomic gases to hot quark gluon plasmas, Rep. Prog. Phys. **72**, 126001 (2009).

[10] P. Kovtun, D. T. Son, and A. O. Starinets, Viscosity in strongly interacting quantum field theories from black hole physics, Phys. Rev. Lett. **94**, 111601 (2005), in the $SU(3)$ pure gauge theory.

[11] S. Gavin and M. Abdel-Aziz, Measuring Shear Viscosity Using Transverse Momentum Correlations in Relativistic Nuclear Collisions, Phys. Rev. Lett. **97**, 162302 (2006).

[12] A. Nakamura and S. Sakai, Transport Coefficients of Gluon Plasma, Phys. Rev. Lett. **94**, 072305 (2005).

[13] H. Song and U. Heinz, Extracting the QGP viscosity from RHIC data: A status report from viscous hydrodynamics, J. Phys. G **36**, 064033 (2009).

[14] H. B. Meyer, A Calculation of the Bulk Viscosity in $SU(3)$ Gluodynamics, Phys. Rev. Lett. **100**, 162001 (2008).

[15] L. P. Csernai, J. I. Kapusta, and L. D. McLerran, On the Strongly-Interacting Low-Viscosity Matter Created in Relativistic Nuclear Collisions, Phys. Rev. Lett. **97**, 152303 (2006).

[16] R. A. Lacey, N. N. Ajitanand, J. M. Alexander, P. Chung, W. G. Holzmann, M. Issah, A. Taranenko, P. Danielewicz, and H. Stöcker, Has the QCD Critical Point Been Signaled by Observations at RHIC?, Phys. Rev. Lett. **98**, 092301 (2007).

[17] F. Karsch, D. Kharzeev, and K. Tuchin, Universal properties of bulk viscosity near the QCD phase transition, Phys. Lett. B **663**, 217 (2008).

[18] K. Paech and S. Pratt, Origins of bulk viscosity in relativistic heavy ion collisions, Phys. Rev. C **74**, 014901 (2006).

[19] J. I. Kapusta and J. M. Torres-Rincon, Thermal conductivity and chiral critical point in heavy ion collisions, Phys. Rev. C **86**, 054911 (2012).

[20] W. T. Deng and X. G. Huang, Event-by-event generation of electromagnetic fields in heavy-ion collisions, Phys. Rev. C **85**, 044907 (2012).

[21] B. G. Zakharov, Electromagnetic response of quark-gluon plasma in heavy-ion collisions, Phys. Lett. B **737**, 262 (2014).

[22] J. Crossno *et al.*, Observation of the Dirac fluid and the break down of the Wiedemann-Franz law in graphene, Science **351**, 1058 (2016).

[23] A. Harutyunyan, D. H. Rischke, and A. Sedrakian, Transport coefficients of two-flavor quark matter from the Kubo formalism, Phys. Rev. D **95**, 114021 (2017).

[24] D. T. Son and A. O. Starinets, Hydrodynamics of r-charged black holes, J. High Energy Phys. 03 (2006) 052.

[25] M. Rangamani, S. F. Ross, D. T. Son, and E. G. Thompson, Conformal non-relativistic hydrodynamics from gravity, J. High Energy Phys. 01 (2009) 075.

[26] M. Braby, J. Chao, and T. Schfer, Thermal conductivity and sound attenuation in dilute atomic Fermi gases, Phys. Rev. A **82**, 033619 (2010).

[27] A. Puglisi, S. Plumari, and V. Greco, Shear viscosity η to electric conductivity σ_{el} ratio for the quark-gluon plasma, Phys. Lett. B **751**, 326 (2015).

[28] P. Danielewicz and M. Gyulassy, Dissipative phenomena in quark gluon plasmas, Phys. Rev. D **31**, 53 (1985).
[29] G. Baym, H. Monien, C. J. Pethick, and D. G. Ravenhall, Transverse Interactions and Transport in Relativistic Quark-Gluon and Electromagnetic Plasmas, Phys. Rev. Lett. **64**, 1867 (1990).
[30] M. H. Thoma, Viscosity coefficient of the quark-gluon plasma in the weak coupling limit, Phys. Lett. B **269**, 144 (1991).
[31] H. Heiselberg and C. J. Pethick, Transport and relaxation in degenerate quark plasmas, Phys. Rev. D **48**, 2916 (1993).
[32] A. Hosoya and K. Kajantie, Transport coefficients of QCD matter, Nucl. Phys. **B250**, 666 (1985).
[33] P. B. Arnold, G. D. Moore, and L. G. Yaffe, Transport coefficients in high temperature gauge theories: 1. Leading log results, J. High Energy Phys. 11 (2000) 001; Transport coefficients in high temperature gauge theories: 2. Beyond leading log, J. High Energy Phys. 05 (2003) 051.
[34] J. W. Chen, H. Dong, K. Ohnishi, and Q. Wang, Shear viscosity of a gluon plasma in perturbative QCD, Phys. Lett. B **685**, 277 (2010); J. W. Chen, J. Deng, H. Dong, and Q. Wang, Shear and bulk viscosities of a gluon plasma in perturbative QCD: Comparison of different treatments for the $gg \to ggg$ process, Phys. Rev. C **87**, 024910 (2013).
[35] A. S. Khvorostukhin, V. D. Toneev, and D. N. Voskresensky, Shear and bulk viscosities for pure glue matter, Phys. Rev. C **83**, 035204 (2011).
[36] Z. Xu and C. Greiner, Shear Viscosity in a Gluon Gas, Phys. Rev. Lett. **100**, 172301 (2008); Z. Xu, C. Greiner, and H. Stocker, PQCD Calculations of Elliptic Flow and Shear Viscosity at RHIC, Phys. Rev. Lett. **101**, 082302 (2008).
[37] T. Schaefer, Fluid dynamics and viscosity in strongly correlated fluids, Annu. Rev. Nucl. Part. Sci. **64**, 125 (2014).
[38] S. Jeon and L. G. Yaffe, From quantum field theory to hydrodynamics: Transport coefficients and effective kinetic theory, Phys. Rev. D **53**, 5799 (1996).
[39] S. Jeon, Hydrodynamic transport coefficients in relativistic scalar field theory, Phys. Rev. D **52**, 3591 (1995); A. Hosoya, M.-a. Sakagami, and M. Takao, Nonequilibrium thermodynamics in field theory: Transport coefficients, Ann. Phys. (N.Y.) **154**, 229 (1984); M. E. Carrington, D.-f. Hou, and R. Kobes, Shear viscosity in ϕ^4 theory from an extended ladder resummation, Phys. Rev. D **62**, 025010 (2000); M. A. Valle Basagoiti, Transport coefficients and ladder summation in hot gauge theories, Phys. Rev. D **66**, 045005 (2002); G. D. Moore and O. Saremi, Bulk viscosity and spectral functions in QCD, J. High Energy Phys. 09 (2008) 015.
[40] C. Sasaki and K. Redlich, Transport coefficients near chiral phase transition, Nucl. Phys. **A832**, 62 (2010); P. Deb, G. P. Kadam, and H. Mishra, Estimating transport coefficients in hot and dense quark matter, Phys. Rev. D **94**, 094002 (2016); S. Ghosh, T. C. Peixoto, V. Roy, F. E. Serna, and G. Krein, Shear and bulk viscosities of quark matter from quark-meson fluctuations in the Nambu–Jona-Lasinio model, Phys. Rev. C **93**, 045205 (2016); S. Ghosh, A. Lahiri, S. Majumder, R. Ray, and S. K. Ghosh, Shear viscosity due to Landau damping from the quark-pion interaction, Phys. Rev. C **88**, 068201 (2013).
[41] S. Plumari, A. Puglisi, F. Scardina, and V. Greco, Shear viscosity of a strongly interacting system: Green-Kubo vs. Chapman-Enskog and relaxation time approximation, Phys. Rev. C **86**, 054902 (2012).
[42] V. Chandra, Transport properties of anisotropically expanding quark-gluon plasma within a quasi-particle model, Phys. Rev. D **86**, 114008 (2012); On the bulk viscosity of anisotropically expanding hot QCD plasma, Phys. Rev. D **84**, 094025 (2011).
[43] G. Denicol, A. Monnai, and B. Schenke, Moving Forward to Constrain the Shear Viscosity of QCD Matter, Phys. Rev. Lett. **116**, 212301 (2016).
[44] S. Ryu, J.-F. Paquet, C. Shen, G. S. Denicol, B. Schenke, S. Jeon, and C. Gale, Importance of the Bulk Viscosity of QCD in Ultrarelativistic Heavy-Ion Collisions, Phys. Rev. Lett. **115**, 132301 (2015).
[45] T. Hirano and M. Gyulassy, Perfect fluidity of the quark gluon plasma core as seen through its dissipative hadronic corona, Nucl. Phys. **A769**, 71 (2006).
[46] B. A. Gelman, E. V. Shuryak, and I. Zahed, Classical strongly coupled QGP: I. The model and molecular dynamics simulations, Phys. Rev. C **74**, 044908 (2006).
[47] S. K. Chakrabarti, S. Jain, and S. Mukherji, Viscosity to entropy ratio at extremality, J. High Energy Phys. 01 (2010) 068; G. Policastro, D. T. Son, and A. O. Starinets, The Shear Viscosity of Strongly Coupled $N = 4$ Supersymmetric Yang-Mills Plasma, Phys. Rev. Lett. **87**, 081601 (2001); S. Cremonini, The shear viscosity to entropy ratio: A status report, Mod. Phys. Lett. B **25**, 1867 (2011); S. Cremonini, U. Gursoy, and P. Szepietowski, On the temperature dependence of the shear viscosity and holography, J. High Energy Phys. 08 (2012) 167; A. Buchel and S. Cremonini, Viscosity bound and causality in superfluid plasma, J. High Energy Phys. 10 (2010) 026; S. Cremonini and P. Szepietowski, Generating temperature flow for η/s with higher derivatives: From Lifshitz to AdS, J. High Energy Phys. 02 (2012) 038; D. Li, S. He, and M. Huang, Temperature dependent transport coefficients in a dynamical holographic QCD model, J. High Energy Phys. 06 (2015) 046; A. Buchel, Bulk viscosity of gauge theory plasma at strong coupling, Phys. Lett. B **663**, 286 (2008).
[48] M. Greif, F. Reining, I. Bouras, G. S. Denicol, Z. Xu, and C. Greiner, Heat conductivity in relativistic systems investigated using a partonic cascade, Phys. Rev. E **87**, 033019 (2013).
[49] R. Marty, E. Bratkovskaya, W. Cassing, J. Aichelin, and H. Berrehrah, Transport coefficients from the Nambu–Jona-Lasinio model for $SU(3)_f$, Phys. Rev. C **88**, 045204 (2013).
[50] S.-i. Nam, Thermal conductivity of the quark matter for the $SU(2)$ light-flavor sector, Mod. Phys. Lett. A **30**, 1550054 (2015).
[51] M. Greif, I. Bouras, C. Greiner, and Z. Xu, Electric conductivity of the quark-gluon plasma investigated using a perturbative QCD based parton cascade, Phys. Rev. D **90**, 094014 (2014).
[52] A. Puglisi, S. Plumari, and V. Greco, Electric conductivity of the QGP, J. Phys. Conf. Ser. **612**, 012057 (2015).
[53] W. Cassing, O. Linnyk, T. Steinert, and V. Ozvenchuk, Electrical Conductivity of Hot QCD Matter, Phys. Rev. Lett. **110**, 182301 (2013).

[54] T. Steinert and W. Cassing, Electric and magnetic response of hot QCD matter, Phys. Rev. C **89**, 035203 (2014).
[55] S.-x. Qin, A divergence-free method to extract observables from correlation functions, Phys. Lett. B **742**, 358 (2015).
[56] P. K. Srivastava, L. Thakur, and B. K. Patra, Electrical conductivity of an anisotropic quark gluon plasma: A quasiparticle approach, Phys. Rev. C **91**, 044903 (2015).
[57] S. Mitra and V. Chandra, Thermal relaxation, electrical conductivity, and charge diffusion in a hot QCD medium, Phys. Rev. D **94**, 034025 (2016).
[58] Y. Yin, Electrical conductivity of the quark-gluon plasma and soft photon spectrum in heavy-ion collisions, Phys. Rev. C **90**, 044903 (2014).
[59] A. Amato, G. Aarts, C. Allton, P. Giudice, S. Hands, and J. I. Skullerud, Electrical Conductivity of the Quark-Gluon Plasma across the Deconfinement Transition, Phys. Rev. Lett. **111**, 172001 (2013).
[60] G. Aarts, C. Allton, A. Amato, P. Giudice, S. Hands, and J. I. Skullerud, Electrical conductivity and charge diffusion in thermal QCD from the lattice, J. High Energy Phys. 02 (2015) 186.
[61] G. Aarts, C. Allton, J. Foley, S. Hands, and S. Kim, Spectral Functions at Small Energies and the Electrical Conductivity in Hot, Quenched Lattice QCD, Phys. Rev. Lett. **99**, 022002 (2007).
[62] S. Gupta, The electrical conductivity and soft photon emissivity of the QCD plasma, Phys. Lett. B **597**, 57 (2004).
[63] B. B. Brandt, A. Francis, H. B. Meyer, and H. Wittig, Thermal correlators in the ρ channel of two-flavor QCD, J. High Energy Phys. 03 (2013) 100; Two-flavour lattice QCD correlation functions in the deconfinement transition region, *Proc. Sci.*, ConfinementX (2012) 186.
[64] H.-T. Ding, A. Francis, O. Kaczmarek, F. Karsch, E. Laermann, and W. Soeldner, Thermal dilepton rate and electrical conductivity: An analysis of vector current correlation functions in quenched lattice QCD, Phys. Rev. D **83**, 034504 (2011).
[65] A. Francis and O. Kaczmarek, On the temperature dependence of the electrical conductivity in hot quenched lattice QCD, Prog. Part. Nucl. Phys. **67**, 212 (2012).
[66] S. Jain, Universal thermal and electrical conductivity from holography, J. High Energy Phys. 11 (2010) 092; Universal properties of thermal and electrical conductivity of gauge theory plasmas from holography, J. High Energy Phys. 06 (2010) 023; Holographic electrical and thermal conductivity in strongly coupled gauge theory with multiple chemical potentials, J. High Energy Phys. 03 (2010) 101; S. I. Finazzo and R. Rougemont, Thermal photon, dilepton production, and electric charge transport in a baryon rich strongly coupled QGP from holography, Phys. Rev. D **93**, 034017 (2016); S. Caron-Huot, P. Kovtun, G. D. Moore, A. Starinets, and L. G. Yaffe, Photon and dilepton production in supersymmetric Yang-Mills plasma, J. High Energy Phys. 12 (2006) 015; Y. Bu, M. Lublinsky, and A. Sharon, $U(1)$ current from the AdS/CFT: Diffusion, conductivity and causality, J. High Energy Phys. 04 (2016) 136; R. Rougemont, J. Noronha, and J. Noronha-Hostler, Suppression of Baryon Diffusion and Transport in a Baryon Rich Strongly Coupled Quark-Gluon Plasma, Phys. Rev. Lett. **115**, 202301 (2015); S. I. Finazzo, R. Rougemont, H. Marrochio, and J. Noronha, Hydrodynamic transport coefficients for the non-conformal quark-gluon plasma from holography, J. High Energy Phys. 02 (2015) 051.
[67] V. Chandra and V. Ravishankar, A quasi-particle description of $(2+1)$-flavor lattice QCD equation of state, Phys. Rev. D **84**, 074013 (2011).
[68] A. Peshier, B. Kampfer, O. P. Pavlenko, and G. Soff, An effective model of the quark-gluon plasma with thermal parton masses, Phys. Lett. B **337**, 235 (1994); A. Peshier, B. Kampfer, and G. Soff, The equation of state of deconfined matter at finite chemical potential in a quasiparticle description, Phys. Rev. C **61**, 045203 (2000); From QCD lattice calculations to the equation of state of quark matter, Phys. Rev. D **66**, 094003 (2002); V. M. Bannur, Self-consistent quasiparticle model for quark-gluon plasma, Phys. Rev. C **75**, 044905 (2007); Self-consistent quasiparticle model for 2, 3 and $(2+1)$ flavor QGP, Phys. Rev. C **78**, 045206 (2008); Quasi-particle model for QGP with nonzero densities, J. High Energy Phys. 09 (2007) 046; A. Rebhan and P. Romatschke, HTL quasiparticle models of deconfined QCD at finite chemical potential, Phys. Rev. D **68**, 025022 (2003); M. A. Thaler, R. A. Schneider, and W. Weise, Quasiparticle description of hot QCD at finite quark chemical potential, Phys. Rev. C **69**, 035210 (2004); K. K. Szabo and A. I. Toth, Quasiparticle description of the QCD plasma, comparison with lattice results at finite T and μ, J. High Energy Phys. 06 (2003) 008.
[69] M. D'Elia, A. Di Giacomo, and E. Meggiolaro, Field strength correlators in full QCD, Phys. Lett. B **408**, 315 (1997); Gauge invariant field strength correlators in pure Yang-Mills and full QCD at finite temperature, Phys. Rev. D **67**, 114504 (2003); P. Castorina and M. Mannarelli, Effective degrees of freedom and gluon condensation in the high temperature deconfined phase, Phys. Rev. C **75**, 054901 (2007); Effective degrees of freedom of the quark-gluon plasma, Phys. Lett. B **644**, 336 (2007); P. Alba, W. Alberico, M. Bluhm, V. Greco, C. Ratti, and M. Ruggieri, Polyakov loop and gluon quasiparticles: A self-consistent approach to Yang-Mills thermodynamics, Nucl. Phys. **A934**, 41 (2014).
[70] A. Dumitru and R. D. Pisarski, Degrees of freedom and the deconfining phase transition, Phys. Lett. B **525**, 95 (2002); K. Fukushima, Chiral effective model with the Polyakov loop, Phys. Lett. B **591**, 277 (2004); S. K. Ghosh, T. K. Mukherjee, M. G. Mustafa, and R. Ray, Susceptibilities and speed of sound from PNJL model, Phys. Rev. D **73**, 114007 (2006); H. Abuki and K. Fukushima, Gauge dynamics in the PNJL model: Color neutrality and Casimir scaling, Phys. Lett. B **676**, 57 (2009).
[71] M. Cheng *et al.*, The QCD equation of state with almost physical quark masses, Phys. Rev. D **77**, 014511 (2008).
[72] A. Bazavov *et al.*, Equation of state and QCD transition at finite temperature, Phys. Rev. D **80**, 014504 (2009); M. Cheng *et al.*, Equation of state for physical quark masses, Phys. Rev. D **81**, 054504 (2010); S. Borsanyi, G. Endrodi, Z. Fodor, A. Jakovac, S. D. Katz, S. Krieg, C.

Ratti, and K. K. Szabo, The QCD equation of state with dynamical quarks, J. High Energy Phys. 11 (2010) 077; S. Borsányi, Z. Fodor, C. Hoelbling, S. D. Katz, S. Krieg, C. Ratti, and K. K. Szabó (Wuppertal-Budapest Collaboration), Is there still any T_c mystery in lattice QCD? Results with physical masses in the continuum limit III, J. High Energy Phys. 09 (2010) 073.

[73] P. B. Arnold and C. X. Zhai, The three loop free energy for pure gauge QCD, Phys. Rev. D **50**, 7603 (1994).

[74] P. B. Arnold and C. X. Zhai, The three loop free energy for high temperature QED and QCD with fermions, Phys. Rev. D **51**, 1906 (1995).

[75] C. X. Zhai and B. M. Kastening, The Free energy of hot gauge theories with fermions through g^5, Phys. Rev. D **52**, 7232 (1995).

[76] K. Kajantie, M. Laine, K. Rummukainen, and Y. Schroder, The Pressure of hot QCD up to $g^6 \ln(1/g)$, Phys. Rev. D **67**, 105008 (2003).

[77] P. F. Kelly, Q. Liu, C. Lucchesi, and C. Manuel, Deriving the Hard Thermal Loops of QCD from Classical Transport Theory, Phys. Rev. Lett. **72**, 3461 (1994); Classical transport theory and hard thermal loops in the quark-gluon plasma, Phys. Rev. D **50**, 4209 (1994); D. F. Litim and C. Manuel, Semiclassical transport theory for non-Abelian plasmas, Phys. Rep. **364**, 451 (2002); J. P. Blaizot and E. Iancu, The quark gluon plasma: Collective dynamics and hard thermal loops, Phys. Rep. **359**, 355 (2002).

[78] V. Chandra and V. Ravishankar, Quasi-particle model for lattice QCD: Quark-gluon plasma in heavy ion collisions, Eur. Phys. J. C **64**, 63 (2009); Viscosity and thermodynamic properties of QGP in relativistic heavy ion collisions, Eur. Phys. J. C **59**, 705 (2009); V. Chandra and V. Sreekanth, Quark and gluon distribution functions in a viscous quark-gluon plasma medium and dilepton production via $q\bar{q}$ annihilation, Phys. Rev. D **92**, 094027 (2015); Impact of momentum anisotropy and turbulent chromo-fields on thermal particle production in quark-gluon plasma medium, Eur. Phys. J. C **77**, 427 (2017); V. Chandra and V. Ravishankar, Quarkonia in anisotropic hot QCD medium in a quasi-particle model, Nucl. Phys. **A848**, 330 (2010); V. Chandra and S. K. Das, Impact of momentum-space anisotropy on heavy quark dynamics in a QGP medium, Phys. Rev. D **93**, 094036 (2016); S. K. Das, V. Chandra, and J.-e. Alam, Heavy-quark transport coefficients in a hot viscous quark gluon plasma medium, J. Phys. G **41**, 015102 (2014).

[79] M. Albright and J. I. Kapusta, Quasiparticle theory of transport coefficients for hadronic matter at finite temperature and baryon density, Phys. Rev. C **93**, 014903 (2016).

[80] M. Bluhm, B. Kampfer, and K. Redlich, Bulk and shear viscosities of the gluon plasma in a quasiparticle description, Phys. Rev. C **84**, 025201 (2011).

[81] P. Chakraborty and J. I. Kapusta, Quasi-particle theory of shear and bulk viscosities of hadronic matter, Phys. Rev. C **83**, 014906 (2011).

[82] K. Dusling and T. Schafer, Bulk viscosity, particle spectra, and flow in heavy-ion collisions, Phys. Rev. C **85**, 044909 (2012).

[83] Sangyong Jeon, Hydrodynamic transport coefficients in relativistic scalar field theory, Phys. Rev. D **52**, 3591 (1995).

[84] M. Alqahtani, M. Nopoush, and M. Strickland, Quasiparticle anisotropic hydrodynamics for central collisions, Phys. Rev. C **95**, 034906 (2017).

[85] V. Chandra and V. Ravishankar, Quasi-particle model for lattice QCD: Quark-gluon plasma in heavy ion collisions, Eur. Phys. J. C **64**, 63 (2009).

[86] X. F. Zhang and W. Q. Chao, Thermal relaxation time in chemically nonequilibrated quark-gluon plasma, Nucl. Phys. **A628**, 161 (1998).

[87] B. L. Combridge, J. Kripfganz, and J. Ranft, Hadron production at large transverse momentum and QCD, Phys. Lett. **70B**, 234 (1977).

[88] M. H. Thoma, Parton interaction rates in the quark-gluon plasma, Phys. Rev. D **49**, 451 (1994).

[89] W. A. Van Leeuwen, P. H. Polak, and S. R. De Groot, On relativistic kinetic gas theory IX: Transport coefficients for systems of particles with arbitrary interaction, Physica (Amsterdam) **66**, 455 (1973).

[90] S. Weinberg, Entropy generation and the survival of protogalaxies in an expanding universe, Astrophys. J. **168**, 175 (1971).

[91] X.-H. Ge, Y. Ling, C. Niu, and S.-J. Sin, Thermoelectric conductivities, shear viscosity, and stability in an anisotropic linear axion model, Phys. Rev. D **92**, 106005 (2015).

[92] M. Braby, J. Chao, and T. Schäfer, Thermal conductivity and sound attenuation in dilute atomic Fermi gases, Phys. Rev. A **82**, 033619 (2010).

[93] Z. Xu and C. Greiner, Thermalization of gluons in ultrarelativistic heavy ion collisions by including three-body interactions in a parton cascade, Phys. Rev. C **71**, 064901 (2005).

[94] P. B. Arnold, C. Dogan, and G. D. Moore, The bulk viscosity of high-temperature QCD, Phys. Rev. D **74**, 085021 (2006).

[95] P. L. Bhatnagar, E. P. Gross, and M. Krook, A model for collision processes in gases: 1. Small amplitude processes in charged and neutral one-component systems, Phys. Rev. **94**, 511 (1954).

[96] J. I. Kapusta, B. Muller, and M. Stephanov, Relativistic theory of hydrodynamic fluctuations with applications to heavy ion collisions, Phys. Rev. C **85**, 054906 (2012).